haematologica
Journal of the Ferrata Storti Foundation

Binding of therapeutic Fc-fused factor VIII to the neonatal Fc receptor at neutral pH associates with poor half-life extension

by Alejandra Reyes-Ruiz, Sandrine Delignat, Aishwarya Sudam Bhale, Victoria Daventure, Robin V. Lacombe, Leslie Dourthe, Olivier Christophe, Sune Justesen, Krishnan Venkataraman, Jordan D. Dimitrov, and Sebastien Lacroix-Desmazes

Received: August 30, 2024.
Accepted: December 5, 2024.

Citation: Alejandra Reyes-Ruiz, Sandrine Delignat, Aishwarya Sudam Bhale, Victoria Daventure, Robin V. Lacombe, Leslie Dourthe, Olivier Christophe, Sune Justesen, Krishnan Venkataraman, Jordan D. Dimitrov, and Sebastien Lacroix-Desmazes. Binding of therapeutic Fc-fused factor VIII to the neonatal Fc receptor at neutral pH associates with poor half-life extension. Haematologica. 2024 Dec 12. doi: 10.3324/haematol.2024.286536 [Epub ahead of print]

Binding of therapeutic Fc-fused factor VIII to the neonatal Fc receptor at neutral pH associates with poor half-life extension

Alejandra Reyes-Ruiz[1], Sandrine Delignat[1], Aishwarya Sudam Bhale[2], Victoria Daventure[1], Robin V. Lacombe[1], Leslie Dourthe[1], Olivier Christophe[3], Sune Justesen[4], Krishnan Venkataraman[2], Jordan D. Dimitrov[1], Sebastien Lacroix-Desmazes[1]

[1] Institut National de la Santé et de la Recherche Médicale, Centre de Recherche des Cordeliers, CNRS, Sorbonne Université, Université Paris Cité, Paris, France; [2] Centre for Bio-Separation Technology (CBST), Vellore Institute of Technology (VIT), Vellore, Tamil Nadu, India; [3] Laboratory for Hemostasis, Inflammation & Thrombosis, Unité Mixed de Recherche 1176, Institut National de la Santé et de la Recherche Médicale, Université Paris-Saclay, Le Kremlin-Bicêtre, France; [4] Immunitrack Aps, Lersoe Park Alle 42, 2100, Copenhagen East, Denmark.

Running head. Binding of rFVIIIFc to FcRn at neutral pH

Corresponding authors. Sébastien Lacroix-Desmazes. **Email:** sebast ien. lacroix-

desmazes@inserm.fr

Author Contributions. Designed the research: ARR, SD, ASB, KV, JDD, SLD. Performed the experiments: ARR, SD, ASB, LD. Contributed essential material: OC, SJ, RL. Analyzed the results: ARR, SD, ASB, KV, JDD, SLD. Wrote the manuscript: ARR, SD, ASB, SLD

Data availability. All data are included in the paper or in the supplemental information. Additional data will be shared on reasonable request to the corresponding author.

Acknowledgments. ReFacto® and Eloctate® were kind gifts from Novo Nordisk A/S (Måløv, Denmark), and Sanofi-Genzyme (Cambridge, MA)/Swedish Orphan Biovitrum AB (Stockholm, Sweden). We thank to Hugo Mouquet (Institut Pasteur, France), for providing the genes encoding the VL and VH regions of human anti-HIV m66.6 IgG, as well as the staff from “Centre d'Expérimentation Fonctionnelle” and “Centre d’Histologie, d’Imagerie Cellulaire et de Cytométrie (CHIC)”, a member of the Sorbonne Université Cell Imaging and Flow Cytometry network (LUMIC) and UPD cell imaging networks, at Centre de Recherche des Cordeliers (Paris) for assistance.

Funding. This work was supported by Institut National de la Santé et de la Recherche Médicale (INSERM), Centre National de la Recherche Scientifique (CNRS), Sorbonne Université, Université de Paris, Assistance Publique des Hôpitaux de Paris and funded by the European Union's Horizon 2020 research and innovation program under the Marie Sklodowska-Curie grant agreement n°859974 (EDUC8) and by grants from Agence National de la Recherche (ANR-18-CE17-0010-02, n°18181LL, Exfiltrins), Sanofi-Genentech (Waltham, MA) and (Swedish Orphan Biovitrum AB (Höllviksnäs, Sweden). ARR was recipient of fellowships from MSCA-ITN EDUC8 (n°859974) and from FRM (FDT202304016725*)*. KV acknowledges the receipt of VTT International Research Found (Ref No. VIN/2022-23/011 dated February 9, 2023).

Declaration of interest: SLD is co-inventor in two patents related to Fc-fused proteins (US20220175896A1 and US20170072032A1). Other authors have no conflict of interest

Abstract

Fusion of therapeutic proteins to the Fc fragment of human IgG1 promotes their FcRn-mediated recycling and subsequent extension in circulating half-life. However, different Fc-fused proteins, as well as antibodies with different variable domains but identical Fc, may differ in terms of extension in half-life. Here we compared the binding behaviour to FcRn of Fc-fused FVIII, Fc-fused FIX and two human monoclonal HIV-1 broadly-neutralizing IgG1, m66.6 and VRC01 with identical Fc. While all molecules bound FcRn at acidic pH, only rFVIIIFc and m66.6 interacted with FcRn at neutral pH. In silico modelling predicted a role for charged residues in the C1 and C2 domains of FVIII, and in the variable domains of m66.6, in the neutral binding to FcRn. Accordingly, mutations of key positively charged amino-acids in the FVIII C1C2 domains decreased the binding of the protein to FcRn at pH 7.4 in vitro and increased the half-life of rFVIIIFc in VWF-KO mice. Our findings suggest that the removal of positively charged patches on Fc-fused proteins to ameliorate FcRn recycling without affecting therapeutic efficacy, may improve their pharmacokinetic properties.

Key Points

1. rFVIIIFc binds FcRn at neutral pH through the C domains of its FVIII moiety

2. Reduction of the positive electrostatic potential of the rFVIIIFc C domains lowers FcRn binding and increases its half-life in VWF-KO mice

Keywords: neonatal Fc receptor, Factor VIII, Fc-fused FVIII, Hemophilia A

Introduction

Immunoglobulins of the IgG isotype are among the circulating proteins with the longest half-life. IgG from humans, non-human primates and mice have half-lives of 7-21,[1] 8-9[2] and 6-8 days,[3] respectively. Such long half-lives are mediated by binding of the "constant" crystallizable fragment (Fc) of the IgG to the neonatal Fc receptor (FcRn).[4] Following pinocytosis, IgG reach early endosomes. Upon progressive acidification in the intra-endosomal space, the imidazole side chains of histidines in the IgG Fc fragments gain positive charges and promote the binding of the Fc I253, T254, H310, H433 and H435 residues to the negatively charged E115, E116, D130 and E133 residues of FcRn.[5] Such interactions rescue IgG from lysosomal degradation and favor their recycling at the cell surface and release in the circulation at neutral pH.[5] FcRn-mediated recycling of IgG was exploited as Fc-fusion technology to increase the half-life of therapeutic molecules with poor pharmacokinetics.[6] Importantly, 79% of the FDA approved Fc-fused molecules exhibit half-lives varying from 3 to 14 days.[7–9]

Coagulation factors VIII (FVIII) and IX (FIX) are two relevant examples of therapeutic proteins with short half-lives: 7 to 15 hours (h) with a mean of 11h for FVIII and 29 to 44h, with a mean of 36h for FIX.[10] FVIII and FIX are used as replacement therapy to restore coagulation in patients with hemophilia A (HA) or B, two rare X-linked, recessive bleeding diseases caused by insufficient levels of endogenous FVIII or FIX, respectively. The poor pharmacokinetics of both therapeutic molecules impose twice to trice weekly dosing to ensure sufficient

protein levels and optimal joint protection in patients with the severe forms of the disease.[11] In the last two decades, FVIII and FIX have been engineered by PEGylation,[12,13] albumin-fusion[14] or Fc-fusion technology[15,16] in order to generate products with extended half-lives (EHL). While EHL FIX products achieve significantly longer half-lives (3 to over 5-fold) as compared to the unmodified short-half life (SHL) FIX products, the half-life extension of EHL FVIII products is limited to 1.3 to 1.7-fold as compared to that of SHL FVIII products.[10] Importantly, the limited half-life extension of therapeutic EHL FVIII ties patients with severe HA to life-long prophylactic treatment with dosing frequencies of 2 times per week.[15] The drastic differences in half-life extension observed between Fc-fused FVIII (rFVIIIFc) and Fc-fused FIX (rFIXFc) suggest that both molecules are not recycled to similar extents by the FcRn. Interestingly, differences in pharmacokinetics have also been reported in the case of monoclonal human antibodies (mAbs) that share identical Fc fragments but carry different variable (Fv) regions.[17] Notably, the presence of positively charged amino-acids in the Fv was found to affect FcRn-mediated recycling of some IgG; it favored interactions of the Fv with FcRn at neutral pH, thus preventing extracellular release and fostering lysosomal degradation.[18,19]

The limited increase in half-life of rFVIIIFc has so far been explained by the binding of the FVIII moiety of the therapeutic molecule to its endogenous chaperon, von Willebrand factor (VWF).[20] Under physiological conditions, the interaction of FVIII with VWF protects FVIII from uncontrolled activation and from

interactions with FVIII-specific catabolic receptors.[21–23] It however favors the catabolism of the FVIII/VWF complex by VWF-specific receptors.[24] Yet, additional VWF-independent mechanisms may contribute to limitation in FVIII half-life extension. Indeed, a Fc-fused FVIII that includes the FVIII-binding D'D3 domains of VWF and free FVIII from its dependence on endogenous VWF did not demonstrate increased half-life in FVIII-KO mice:[25] the 35 hour-long half-life of Efanesoctocog alfa was only achieved following introduction of XTEN polypeptides in the molecule.[25]

Here, we investigated whether other mechanisms beyond VWF catabolism could contribute to the short half-life of rFVIIIFc. We observed that rFVIIIFc binds FcRn at neutral pH. The binding was associated with the presence of positively charged residues in the C1 and C2 domains of the FVIII moiety of the molecule. Mutations of key charged amino-acids drastically reduced the binding of rFVIIIFc to FcRn at neutral pH. It further led to a 2.5-fold increased half-life in VWF-deficient mice.

Methods

Sources of Fc-fused molecules. Recombinant Fc-fused FIX (Alprolix®), B domain-deleted (BDD) FVIII (ReFacto AF®) and Fc-fused BDD-FVIII (rFVIIIFc, Eloctate®) were gifts from Sanofi-Genentech and SOBI. The rFVIII^{C1C2}Fc. rFVIII^{N2118Q}Fc mutants were generated by site-directed mutagenesis applying In-Fusion system (Takara) using the cDNA encoding human BDD-FVIII (containing

the SFSQNPPVLKRHQR segment instead of the B domain), and the cDNA encoding a human Fcγ1 domain dimerized with a linker (provided by Sanofi®) as templates. The mutated cDNAs were cloned in the ReNeo plasmid and validated by standard sequencing analysis. The rFVIII^{C1C2}Fc mutant bears the R2090A, K2092A, F2093A, R2215A mutations. BHK-M cells were transfected and selected for neomycin resistant clones using Geneticin-sulfate (500 µg/ml, Sigma-Aldrich, St. Louis, MO). FVIII producing clones were screened using a FVIII chromogenic assay (Siemens Healthcare, Erlangen, Germany). The selected highest expressing clones were scaled up to near confluency before switching the medium to serum free AIM-V medium (Thermo Scientific, Waltham, MA). Medium was collected every 24 hrs; cells were replenished with fresh AIM-V medium. FVIII purification was performed by affinity chromatography on VIIIselect column (GE Healthcare, Chicago, IL), followed by anion-exchange chromatography on HiTrap Resource Q column (GE Healthcare). Purified rFVIIIFc was analyzed by 4–12% SDS-PAGE ± activation by bovine thrombin (Sigma-Aldrich) (**Fig. S1**) and detected by silver staining. The activity of the different purified rFVIIIFc variants was measured using the FVIII chromogenic assay; protein concentrations were measured using nanodrop or Bradford assay (Bio-Rad, Hercules, CA) (**Table S1**). The specific activities were 4265 IU/mg for rFVIIIFc, 1392 to 2398 IU/mg for FVIII^{C1C2}Fc and 1951 IU/mg for FVIII^{N2118Q}Fc (**Table S1**). The study has been approved by a formally constituted review board (Charles Darwin ethics committee #28694-2020121017336521).

Results

Fc-fused FVIII binds to FcRn at physiological pH

The commercially available Fc-fused B domain-deleted (BDD) FVIII (Eloctate®) presents with a limited increase in FVIII half-life over therapeutic BDD FVIII as compared to human IgG and other therapeutic Fc-fused molecules, thus raising questions on its capacity to be recycled by the FcRn following endocytosis. Using real time interaction analyses based on SPR (see supplemental Methods online), we first confirmed that, at pH 6, rFVIIIFc interacts with human and murine FcRn with binding affinities (1.4-2.0 and 0.2-0.3 nM, respectively, **Table 1**) similar to that measured for m66.6 (1.3-2.8 and 0.2-0.4 nM), a human anti-MPER HIV monoclonal IgG.[26] The affinities were slightly higher than that determined for commercially available Fc-fused FIX (rFIXFc, Alprolix®, 2.1-5.0 and 0.3-0.9 nM, respectively)[27] and VRC01 (3.1-5.0 and 0.4-0.9 nM, respectively), a human monoclonal IgG specific for HIV gp120 [28] (**Fig. 1A-B**). These results were confirmed by ELISA. At acidic pH, rFVIIIFc, rFIXFc, m66.6 and VRC01 exhibited similar binding profiles to human or mouse FcRn (**Fig. 1C**). At neutral pH however, rFVIIIFc and m66.6 presented with residual binding to both human and mouse FcRn that was greater than that observed for rFIXFc and VRC01 (**Fig. 2A-B**). By ELISA, rFVIIIFc and m66.6 IgG bound to human and mouse FcRn at pH 7.4 in a dose-dependent manner, while rFIXFc and VRC01 exhibited a weak binding (**Fig. 2C**). The binding of BDD-FVIII without the Fc fragment to human

and mouse FcRn, that was not detected by SPR at pH 7.4 (**Fig.1C**), was evidenced by ELISA with a 50% binding close to 1140 and 130 nM, respectively (**supplementary Fig. S2**).

The C1 and C2 domains of FVIII exhibit a largely positive electrostatic potential

A modeling of the charge distribution on the Fab fragments of m66.6 and VRC01 highlighted a strong positive electrostatic potential for m66.6 (**Fig. 3A)**, that was not present in the case of VRC01 (**Fig. 3B**). Positive charges in the Fv of some human monoclonal IgG have been implicated in their binding to the FcRn at neutral pH and poor pharmacokinetics.[18,19] Our results are in accordance with the latter finding since the presence of positive charges in the Fab fragment of m66.6 was associated with important residual binding to human and mouse FcRn (**Fig. 2**). To get insight into potential reasons for the residual binding of rFVIIIFc to FcRn at neutral pH, we modeled the charge distribution on BDD-FVIII and FcRn. FVIII is a multidomain protein formed of a heavy chain containing the A1a1, A2a2 and B domains, and a light chain containing the a3A3, C1 and C2 domains (**Fig. S3A**).[29] In BDD-FVIII, the C1 and C2 domains exhibited a highly positive electrostatic potential (**Fig. 2C**), as well as a portion of the A3 domain albeit to a lesser extent, reminiscent of the situation with m66.6 Fab (**Fig. 2A**). In contrast, the surface electrostatic potential of FcRn was predominantly negative (**Fig. 3D**), making it an ideal binding partner for the C1 and C2 domains of FVIII.

Charged residues in the FVIII C1 and C2 domains are predicted to promote binding to FcRn

To decipher whether the charge distribution in rFVIIIFc and m66.6 governs binding to FcRn at neutral pH, we studied the effect of variations in ionic strength on FcRn binding by ELISA. The interaction of both molecules with human and mouse FcRn was inhibited in a dose-dependent manner by NaCl concentrations above the physiological value (i.e., 140 mM) and increased with decreasing NaCl concentrations (**Fig. 4A**). As expected, VRC01 and rFIXFc showed a lower binding to FcRn than rFVIIIFc and m66.6, irrespective of the salt concentration. To confirm the implication of the C1 and C2 domains in the binding of rFVIIIFc to FcRn at neutral pH, we measured, by real time interaction analyses at pH 7.4, the binding to FcRn of rFVIIIFc preincubated alone, with VWF to mask its light chain, or with the $F(ab')_2$ fragments of the human monoclonal anti-FVIII IgG KM33, BO2C11, and BOIIB2, that recognize epitopes in the C1[30], C2[31] and A2 (patent US20070065425A1) domains of FVIII, respectively. Of note, rFVIIIFc retained unperturbed binding to VWF as compared to rFVIII by ELISA (**Fig. S4A**). Shielding of rFVIIIFc with VWF almost completely abrogated binding of rFVIIIFc to FcRn (**Fig. 4B**). The protecting effect of VWF was reproduced independently by the anti-C1 and anti-C2 $F(ab')_2$ fragments, confirming the contribution of residues in the latter domains to the binding of rFVIIIFc to FcRn at neutral pH. In contrast, the anti-A2 $F(ab')_2$ fragments did not interfere with rFVIIIFc binding to FcRn (**Fig. 4B**).

The independent FVIII^{C1} and FVIII^{C2} variants containing three mutations in the C1 domain (R2090A, K2092A, F2093A) and one or two mutations in the C2 domain (R2215A and/or R2220A), respectively, lose binding to their cognate antibodies KM33 and BO2C11.[32,33] *In silico* molecular modeling of a FVIII^{C1C2} mutant combining the four mutations (R2090A, K2092A, F2093A, R2215A) suggested that the removal of 3 positively charged residues in the FVIII C1 and C2 domains strikingly decreases the positive electrostatic potential of the FVIII light chain (**Fig. 3C and 4C**).

To further predict the role of these amino-acid residues in the interaction, we conducted domain-specific docking of the C1C2 domain of FVIII to FcRn at neutral pH using the modeled structure of C1C2 **(Fig. S3)** and the HDOCK webserver. The docking yielded a binding score of -282.48, a confidence score of 0.9340, and a ligand RMSD of 124.49 Å. The interaction analysis identified the formation of four hydrogen bonds, two salt bridges, and 204 non-bonded contacts that could be either hydrophobic, van der Waals or electrostatic interactions between the C1C2 domains and FcRn (**Fig. 4D**). Specifically, within the C1 domain, C2021 formed a hydrogen bond with N55 of FcRn, and R2090 formed hydrogen bonds with S181 and P180 of FcRn (**Table 2**). Within the C2 domain, K2207 formed a hydrogen bond with D101 of FcRn. Additionally, two residues from the C2 domain were involved in salt bridge formation: E2181 with R171 of FcRn and K2207 with D101 of FcRn (**Table 2)**. Furthermore, in the C1 domain, R2090, K2092 and F2093 formed non-bonded contacts with P179,

P180, S181 and M182, with R183, and with R183 of FcRn, respectively. In the C2 domain, R2215 formed a non-bonded contact with P100 of FcRn. From the FcRn residues predicted to interact with C1 and C2, W53 (**Table S1, Table 2, Fig. 4D)** was shared with the central residues contributing to albumin interaction.[34] None of the latter residues was shared with the IgG binding site (**Fig. 4D**).[5]

Binding of rFVIIIFc to FcRn at neutral pH is mediated by the FVIII C1 and C2 domains

To confirm the importance of the C1 and C2 residues in the interaction with FcRn at neutral pH, we produced a rFVIII^{C1C2}Fc mutant molecule containing the R2090A, K2092A, F2093A mutations in the C1 domain and the R2215A mutation in the C2 domain. As a control, we produced a rFVIII^{N2118Q}Fc mutant wherein the N-glycosylation site in the C1 domain is removed.[35] In the rFVIII^{C1C2}Fc and rFVIII^{N2118Q}Fc mutants, the Fc fragments are stabilized by a $(GGGGS)_4$ linker. Hence, the migration profile of the molecules slightly differed from that of rFVIIIFc, both when incubated alone and in the presence of thrombin (**Fig. S1**). Besides, the specific activities of rFVIII^{C1C2}Fc (1392-2398 IU/mg, **Table S2**) and rFVIII^{N2118Q}Fc (1951 IU/mg) were lower than that of rFVIIIFc (4265 IU/mg). Both rFVIII^{C1C2}Fc and rFVIII^{N2118Q}Fc retains unperturbed binding to VWF (**Fig. S4A**), reflecting the relative integrity of the light chain structure in the mutated molecules.

At pH 6, rFVIII^{N2118Q}Fc and rFVIII^{C1C2}Fc demonstrated similar binding affinities for FcRn (**Fig. 5A, Table S3**) as assessed by SPR-based kinetics analyses. The affinities were similar to that determined for rFVIIIFc (**Table 1**), suggesting that not all three charged residues contribute to the interaction with FcRn. In agreement, binding ELISA performed at pH 6, revealed identical binding profiles for the three molecules towards mouse and human FcRn (**Fig. S4B**). These data suggest that stabilization of the Fc fragments with a linker, removal of the N-linked glycan in FVIII^{N2118Q}Fc or introduction of mutations in the C1 and C2 domains of rFVIII^{C1C2}Fc do not alter binding to FcRn in acidic conditions.

While, at neutral pH, FVIII^{N2118Q}Fc retained the same binding behavior to FcRn as rFVIIIFc, the rFVIII^{C1C2}Fc mutant demonstrated significantly decreased FcRn binding (**Fig. 5B and 5C**). Similarly, the rFVIII^{C1C2}Fc mutant did not bind to FcRn at neutral pH, irrespective of the salt concentration (**Fig. 5D**), in contrast to rFVIIIFc. Together, the data confirm the contribution of positively charged residues in the FVIII C1 and C2 domains to FcRn binding at physiological pH.

Mutations of charged residues in the C1 and C2 domains of rFVIIIFc increase its half-life in VWF-KO mice

We then evaluated the half-lives of wild-type rFVIIIFc and the engineered FVIII^{C1C2}Fc in mice. The binding of rFVIIIFc to endogenous VWF has been shown to contribute for the largest part to the limited extension in half-life, owing to elimination of the rFVIIIFc/VWF complex by VWF-specific catabolic receptors.[25] In agreement with this, rFVIIIFc and FVIII^{C1C2}Fc exhibited

comparable pharmacokinetics in FVIII-KO mice, with 60 to 70% of the molecules being eliminated in the first hour following injection and the remaining presenting with a half-life ranging from 9.5 to 15.5 hours (**Fig. 6A**). In order to decipher the possible contribution of the binding to FcRn at neutral pH to the half-life of Fc-fused FVIII without the interference of endogenous VWF, we further compared the half-lives of rFVIIIFc and FVIII^{C1C2}Fc in VWF-KO mice. In the absence of endogenous VWF, FVIII^{C1C2}Fc demonstrated a 2.5-fold longer half-life (2.31 hours) than rFVIIIFc (0.94 hours, **Fig. 6B**).

Discussion

Our work demonstrates the binding of rFVIIIFc to FcRn at neutral pH. Because FVIII alone exhibited weak binding affinity for FcRn by ELISA, and because some human IgG1 were documented to bind FcRn at pH 7.4 (see references 36, 37, and patent WO2013046704A2), we hypothesize that the binding of rFVIIIFc to FcRn at neutral pH results from a synergy between the weak binding affinities of the FVIII and Fc moieties of the molecule that leads to consistent augmentation in the binding avidity. The experimental data suggest that the interaction of rFVIIIFc with FcRn is relying on positively charged amino acids residues located in the C1 and/or C2 domains of FVIII. Indeed, reduction of the positive electrostatic potential of C1C2 by mutation of a few key amino-acids was associated with a drastically reduced binding of rFVIIIFc to FcRn at neutral pH and with a statistically relevant increase in circulating half-life of Fc-fused FVIII in

VWF-KO mice. Identifying the amino-acid residue(s) that contribute(s) the most to FcRn binding would require generating individual FVIII^{R2090A}Fc, FVIII^{K2092A}Fc or FVIII^{R2215A}Fc variants. More than 10 therapeutic proteins with FDA authorization exploit the Fc-fusion technology for half-life extension.[38] Among these, procoagulant FVIII, which has an intrinsic mean physiological half-life of about 11 hours,[10] is among the Fc-fused therapeutic proteins with the lowest gain in half-life extension, i.e., 19 hours.[15] This value is significantly lower than that reach by other Fc-fused proteins such as rFIXFc (i.e., 82 hours),[16] the extracellular domain of TNFR fused to Fc (i.e. 70h),[39] Fc-fused CTLA-4 (i.e., 13 days)[7] or therapeutic IgG1 antibodies (i.e., 21 days).[40] Binding of rFVIIIFc to endogenous VWF in the patients' circulation has been identified as a key limitation for its duration in plasma, wherein elimination of the rFVIIIFc/VWF complexes by VWF-specific catabolic pathways imposes a glass ceiling on half-life extension.[25] In this respect, our finding of an interaction of the FVIII light chain of rFVIIIFc with FcRn at neutral pH represents a different molecular mechanism responsible for its limited extension of circulating time in plasma in addition to VWF-mediated mechanism.

Our modelling results confirm a strong positive electrostatic potential of the FVIII C1 and C2 domains, and to a lesser extent of the FVIII A3 domain, and a key role of positively charged amino-acids in establishing contacts with FcRn. The binding of FVIII to the D'D3 domain of VWF implicates both the C1 domain and the acidic a3 peptide through a sulfated tyrosine, while the A3 and C2 domains

play ancillary roles in the interaction.[41] The interaction is essential to maintain FVIII in the circulation and prevent its early catabolism.[21,23] Following its activation by thrombin, FVIII is released from VWF. Subsequently, positively charged residues surrounded by hydrophobic ring of amino acids in the C1 and C2 domains anchor the activated molecule to phospholipids exposed on the surface of activated platelets which fosters the local assembly of the tenase complex together with activated FIX and FX.[42] The C1 and C2 domains also contribute to the interaction of FVIII with the immune system. The two domains are privileged targets for neutralizing anti-FVIII antibodies that develop in a substantial number of hemophilia A patients undergoing FVIII replacement therapy.[43,44] They also mediate the uptake of FVIII by antigen-presenting cells *in vitro*, leading to the processing of FVIII and presentation of FVIII-derived peptides to FVIII-specific CD4+ T lymphocytes.[33,35] The observation of the binding of FVIII C1C2 domains to FcRn extends the array of interactions that the protein may establish at physiological pH.

FcRn-mediated recycling of IgG and Fc-fused proteins involves the endocytosis of the molecules, followed by binding to FcRn at acidic pH in the endosome, transport of the molecules back to the cell surface and release in the circulation upon return to neutral pH.[5] Interference in the process may occur at different levels. The presence of positively charged residues in the Fab fragments of therapeutic IgG was shown to mediate binding to FcRn at neutral pH in an Fc-independent manner.[18,19] Such binding was proposed to interfere with the

release of IgG from FcRn at the end of the recycling process, thus routing the molecules towards lysosomal degradation, and was associated with poor pharmacokinetics. In the case of rFVIIIFc, we observed a similar phenomenon of direct binding to FcRn at neutral pH, suggesting that rFVIIIFc undergoes a similarly impaired release from FcRn upon re-exposure at the cell surface. Interestingly, large IgG-immune complexes (ICs) are excluded from recycling sorting tubules and diverted towards lysosomes.[45] Our *in silico* docking results predicted that the binding surface for FVIII on FcRn is located on the opposite side of FcRn as compared to the Fc-binding surface (i.e., residues E115, E116, D130 and E133).[5] Importantly, the affinities of rFVIIIFc and m66.6 for both human and murine FcRn at acidic pH were moderately greater than that of rFIXFc and VRC01 (Fig. 1A-B, Table 1), as well as rFVIII^{C1C2}Fc (at least in the case of human FcRn). This suggests that the binding of C1C2 detected at neutral pH also occurs at acidic pH (as can be inferred from the conservation of the positive charges upon reduction in pH value) and synergizes with the binding of the Fc fragment to FcRn. Taken together, these data make it plausible that, at acidic pH in the early endosome, rFVIIIFc engages multiple simultaneous interactions with different FcRn molecules, involving both its Fc fragment and its C1 and C2 domains, which would favor routing towards lysosomal disposal immediately after endocytosis.

VWF is the molecular chaperon for circulating FVIII. The crucial role of VWF towards FVIII is best demonstrated in patients with type 2N or type 3 von

Willebrand disease who present with negligible circulating FVIII levels owing to the lack of VWF or presence of dysfunctional VWF.[46,47] Whether VWF also shields FVIII intracellularly is unclear. Sorvillo et al demonstrated that, in contrast to FVIII, VWF is not or poorly endocytosed by human monocyte-derived dendritic cells.[48] Several endocytic receptors for VWF have however been identified on endothelial cells, including C-type lectin domain family 4 member M (CLEC4M), stabilin-2, and scavenger receptor class A member 5 (SCARA5),[49] some of which mediate the internalization of the FVIII-VWF complex. The possibility thus exists that VWF also participates in enhancing the FcRn-mediated intracellular recycling of rFVIIIFc by quenching its positively charged C1 and C2 domains in the endosome and preventing the interaction of C1C2 with FcRn. Indeed, the VWF/FVIII interaction is stable at pH >5.5, at least *in vitro*.[50]

Our modeling of the electrostatic potential of FVIII domains indicated that the positive electrostatic potential of the light chain spreads to part of the A3 domain that is also protected by the D'D3 domain of VWF.[41] In line with this, Efanesoctocog alfa is a recently developed engineered Fc-fused FVIII in complex with the D'D3 domain of VWF with a half-life of 25-31 hours in mice[25] and 33-45 hours in the human.[51] However, the optimal half-life of Efanesoctocog alfa was not reached by the mere addition of the D'D3 domain of VWF, but required the grafting of XTEN polypeptides.[25] At neutral pH, rFVIII^{C1C2}Fc retained a significant binding to FcRn *in vitro*, suggesting the participation of additional positive charges outside the C domains on FVIII in FcRn interaction. Whether the XTEN

polypeptides shield additional positive charges, particularly at the interface between A2 and A3, that are not protected by the D'D3 domain of VWF, and prevent engagement with intracellular receptors, remains to be investigated.

The gain in half-life life of rFVIII^{C1C2}Fc as compared to rFVIIIFc (from 56 to 138 min, Fig. 6B) was only evidenced in the absence of endogenous VWF. Performing similar experiments in transgenic VWF-KO mice expressing the human instead of mouse FcRn may yield more pre-clinically relevant results.[52] Yet, the findings are reminiscent of our previous observation that an increase in half-life from 17 to 41 minutes of the individual FVIII^{C1} and FVIII^{C2} variants was only observed in the absence of endogenous VWF.[33] Interestingly, our previous work showed a reduction in FVIII immunogenicity when the charged residues in the C1 domain of FVIII were mutated. However, once again, this was observed in the absence of endogenous VWF.[33] Whether the reduction of the positive electrostatic potential may be an advantage in the context of FVIII synthesis and intracellular trafficking, where VWF is not at play, needs to be investigated.

In conclusion, we describe an additional mechanism to the VWF-mediated catabolism of rFVIIIFc (**Fig. S5**). The predominant role played by VWF on FVIII catabolism however puts in perspective our findings in terms of translational possibilities. In addition, our attempt to disfavor FVIII binding to FcRn at physiological pH also marginally affected binding to VWF and reduced the specific activity of the molecule, possibly by altering binding to phospholipids. Nonetheless, our data open a mutational space for the reduction of the positive

electrostatic potential of rFVIIIFc, to limit its interactions with molecules that favor its catabolism or prevent its recycling. Besides, complementary strategies may be foreseen to further optimize the half-life of Fc-fused FVIII. For instance, Fc-engineering by introducing the YTE substitutions to strengthen human FcRn interactions was shown to extend the half-life of mAbs with positively charged patches in the Fab fragments.[19] Whether the same strategy may apply to rFVIIIFc, Efanesoctocog alfa, or rFVIII^{C1C2}Fc, remains to be determined. Importantly, beyond the mere example of FVIII, our finding may also be of interest for therapeutic proteins that bear patches with positive net charges and exhibit poor pharmacokinetics.

References

1. Spiegelberg HL, Fishkin BG, Grey HM. Catabolism of human gammaG-immunoglobulins of different heavy chain subclasses. I. Catabolism of gammaG-myeloma proteins in man. J Clin Invest. 1968;47(10):2323-2330.

2. Challacombe SJ, Russell MW. Estimation of the intravascular half-lives of normal rhesus monkey IgG, IgA and IgM. Immunology. 1979;36(2):331-338.

3. Waldmann TA, Strober W. Metabolism of immunoglobulins. Prog Allergy. 1969;13:1-110.

4. Blumberg LJ, Humphries JE, Jones SD, et al. Blocking FcRn in humans reduces circulating IgG levels and inhibits IgG immune complex-mediated immune responses. Sci Adv. 2019;5(12):eaax9586.

5. Martin WL, West AP, Gan L, Bjorkman PJ. Crystal structure at 2.8 A of an FcRn/heterodimeric Fc complex: mechanism of pH-dependent binding. Mol Cell. 2001;7(4):867-877.

6. Pyzik M, Kozicky LK, Gandhi AK, Blumberg RS. The therapeutic age of the neonatal Fc receptor. Nat Rev Immunol. 2023;23(7):415-432.

7. Lutt J. Efficacy, safety, and tolerability of abatacept in the management of rheumatoid arthritis. Open Access Rheumatol. 2009;1:17-35.

8. Shen J, Townsend R, You X, et al. Pharmacokinetics, pharmacodynamics, and immunogenicity of belatacept in adult kidney transplant recipients. Clin Drug Investig. 2014;34(2):117-126.

9. Ipema HJ, Jung MY, Lodolce AE. Romiplostim management of immune thrombocytopenic purpura. Ann Pharmacother, 2009;43(5):914-919.

10. Versloot O, Iserman E, Chelle P, et al. Terminal half-life of FVIII and FIX according to age, blood group and concentrate type: Data from the WAPPS database. J Thromb Haemost, 2021;19(8):1896-1906.

11. Srivastava A, Santagostino E, Dougall A, et al. WFH Guidelines for the Management of Hemophilia, 3rd edition. Haemophilia. 2020;26(S6):1-158.

12. Konkle BA, Stasyshyn O, Chowdary P, et al. Pegylated, full-length, recombinant factor VIII for prophylactic and on-demand treatment of severe hemophilia A. Blood. 2015;126(9):1078-1085.

13. Escuriola Ettingshausen C, Hegemann I, Simpson ML, et al. Favorable pharmacokinetics in hemophilia B for nonacog beta pegol versus recombinant factor IX-Fc fusion protein: A randomized trial. Res Pract Thromb Haemost. 2019;3(2):268-276.

14. Chia J, Louber J, Glauser I, et al. Half-life-extended recombinant coagulation factor IX-albumin fusion protein is recycled via the FcRn-mediated pathway. J Biol Chem. 2018;293(17):6363-6373.

15. Mahlangu J, Powell JS, Ragni MV, et al. Phase 3 study of recombinant factor VIII Fc fusion protein in severe hemophilia A. Blood. 2014;123(3):317-325.

16. Powell JS, Pasi KJ, Ragni MV, et al. Phase 3 study of recombinant factor IX Fc fusion protein in hemophilia B. N Engl J Med. 2013;369(24):2313-2323.

17. Igawa T, Tsunoda H, Tachibana T, et al. Reduced elimination of IgG antibodies by engineering the variable region. Protein Eng Des Sel. 2010;23(5):385-392.

18. Schoch A, Kettenberger H, Mundigl O, et al. Charge-mediated influence of the antibody variable domain on FcRn-dependent pharmacokinetics. Proc Natl Acad Sci U S A. 2015;112(19):5997-6002.

19. Grevys A, Frick R, Mester S, et al. Antibody variable sequences have a pronounced effect on cellular transport and plasma half-life. iScience. 2022;25(2):103746.

20. Pipe SW, Montgomery RR, Pratt KP, Lenting PJ, Lillicrap D. Life in the shadow of a dominant partner: the FVIII-VWF association and its clinical implications for hemophilia A. Blood. 2016;128(16):2007-2016.

21. Fay PJ, Coumans JV, Walker FJ. von Willebrand factor mediates protection of factor VIII from activated protein C-catalyzed inactivation. J Biol Chem. 1991;266(4):2172-2177.

22. Pegon JN, Kurdi M, Casari C, et al. Factor VIII and von Willebrand factor are ligands for the carbohydrate-receptor Siglec-5. Haematologica. 2012;97(12):1855-1863.

23. Nogami K, Shima M, Nishiya K, et al. A novel mechanism of factor VIII protection by von Willebrand factor from activated protein C-catalyzed inactivation. Blood. 2002;99(11):3993-3998.

24. Swystun LL, Lai JD, Notley C, et al. The endothelial cell receptor stabilin-2 regulates VWF-FVIII complex half-life and immunogenicity. J Clin Invest. 2018;128(9):4057-4073.

25. Chhabra ES, Liu T, Kulman J, et al. BIVV001, a new class of factor VIII replacement for hemophilia A that is independent of von Willebrand factor in primates and mice. Blood. 2020;135(17):1484-1496.

26. Zhu Z, Qin HR, Chen W, et al. Cross-Reactive HIV-1-Neutralizing Human Monoclonal Antibodies Identified from a Patient with 2F5-Like Antibodies. J Virol. 2011;85(21):11401-11408.

27. Ducore JM, Miguelino MG, Powell JS. Alprolix (recombinant Factor IX Fc fusion protein): extended half-life product for the prophylaxis and treatment of hemophilia B. Expert Rev Hematol. 2014;7(5):559-571.

28. Ledgerwood JE, Coates EE, Yamshchikov G, et al. Safety, pharmacokinetics and neutralization of the broadly neutralizing HIV-1 human monoclonal antibody VRC01 in healthy adults. Clin Exp Immunol. 2015;182(3):289-301.

29. Lenting PJ, Van Mourik JA, Mertens K. The Life Cycle of Coagulation Factor VIII in View of Its Structure and Function. Blood. 1998;92(11):3983-3996.

30. van den Brink EN, Turenhout EA, Bovenschen N, et al. Multiple VH genes are used to assemble human antibodies directed toward the A3-C1 domains of factor VIII. Blood. 2001;97(4):966-972.

31. Jacquemin MG, Desqueper BG, Benhida A, et al. Mechanism and kinetics of factor VIII inactivation: study with an IgG4 monoclonal antibody derived from a hemophilia A patient with inhibitor. Blood. 1998;92(2):496-506.

32. Wroblewska A, van Haren SD, Herczenik E, et al. Modification of an exposed loop in the C1 domain reduces immune responses to factor VIII in hemophilia A mice. Blood. 2012;119(22):5294-5300.

33. Gangadharan B, Ing M, Delignat S, et al. The C1 and C2 domains of blood coagulation factor VIII mediate its endocytosis by dendritic cells. Haematologica. 2017;102(2):271-281.

34. Sand KMK, Dalhus B, Christianson GJ, et al. Dissection of the Neonatal Fc Receptor (FcRn)-Albumin Interface Using Mutagenesis and Anti-FcRn Albumin-blocking Antibodies. J Biol Chem. 2014;289(24):17228-17239.

35. Delignat S, Rayes J, Dasgupta S, et al. Removal of Mannose-Ending Glycan at Asn2118 Abrogates FVIII Presentation by Human Monocyte-Derived Dendritic Cells. Front Immunol. 2020;11:393.

36. Dumet C, Pugnière M, Henriquet C, Gouilleux-Gruart V, Poupon A, Watier H. Harnessing Fc/FcRn Affinity Data from Patents with Different Machine Learning Methods. Int J Mol Sci. 2023;24(6):5724.

37. Rossini S, Noé R, Daventure V, Lecerf M, Justesen S, Dimitrov JD. V Region of IgG Controls the Molecular Properties of the Binding Site for Neonatal Fc Receptor. J Immunol. 2020;205(10):2850-2860.

38. Duivelshof BL, Murisier A, Camperi J, et al. Therapeutic Fc-fusion proteins: Current analytical strategies. J Sep Sci. 2021;44(1):35-62.

39. Nestorov I, Zitnik R, DeVries T, Nakanishi AM, Wang A, Banfield C. Pharmacokinetics of subcutaneously administered etanercept in subjects with psoriasis. Br J Clin Pharma. 2006;62(4):435-445.

40. Ko S, Jo M, Jung ST. Recent Achievements and Challenges in Prolonging the Serum Half-Lives of Therapeutic IgG Antibodies Through Fc Engineering. BioDrugs. 2021;35(2):147-157.

41. Chiu P-L, Bou-Assaf GM, Chhabra ES, et al. Mapping the interaction between factor VIII and von Willebrand factor by electron microscopy and mass spectrometry. Blood 2015;126(8):935-938.

42. Panteleev MA, Ananyeva NM, Greco NJ, Ataullakhanov FI, Saenko EL. Factor VIIIa regulates substrate delivery to the intrinsic factor X-activating complex. FEBS J. 2006;273(2):374-387.

43. Meeks SL, Healey JF, Parker ET, Barrow RT, Lollar P. Antihuman factor VIII C2 domain antibodies in hemophilia A mice recognize a functionally complex continuous spectrum of epitopes dominated by inhibitors of factor VIII activation. Blood. 2007;110(13):4234-4242.

44. Batsuli G, Deng W, Healey JF, et al. High-affinity, noninhibitory pathogenic C1 domain antibodies are present in patients with hemophilia A and inhibitors. Blood. 2016;128(16):2055-2067.

45. Weflen AW, Baier N, Tang Q-J, et al. Multivalent immune complexes divert FcRn to lysosomes by exclusion from recycling sorting tubules. Mol Biol Cell. 2013;24(15):2398-2405.

46. Mazurier C, Goudemand J, Hilbert L, Caron C, Fressinaud E, Meyer D. Type 2N von Willebrand disease: clinical manifestations, pathophysiology, laboratory diagnosis and molecular biology. Best Pract Res Clin Haematol. 2001;14(2):337-347.

47. Adjambri AE, Bouvier S, N'guessan R, et al. Discovery of Type 3 von Willebrand Disease in a Cohort of Patients with Suspected Hemophilia A in Côte d'Ivoire. Mediterr J Hematol Infect Dis. 2020;12(1):e2020019.

48. Sorvillo N, Hartholt RB, Bloem E, et al. von Willebrand factor binds to the surface of dendritic cells and modulates peptide presentation of factor VIII. Haematologica. 2016;101(3):309-318.

49. Swystun LL, Lillicrap D. Current Understanding of Inherited Modifiers of FVIII Pharmacokinetic Variation. Pharmgenomics Pers Med. 2023;16:239-252.

50. Dimitrov JD, Christophe OD, Kang J, et al. Thermodynamic analysis of the interaction of factor VIII with von Willebrand factor. Biochemistry. 2012;51(20):4108-4116.

51. Konkle BA, Shapiro AD, Quon DV, et al. BIVV001 Fusion Protein as Factor VIII Replacement Therapy for Hemophilia A. N Engl J Med. 2020;383(11):1018-1027.

52. Roopenian DC, Christianson GJ, Sproule TJ. Human FcRn transgenic mice for pharmacokinetic evaluation of therapeutic antibodies. Methods Mol Biol. 2010;602:93-104.

Tables

Table 1. Kinetic parameters for the binding of Fc-fused molecules or antibodies to human and mouse FcR at pH 6.

	Binding to human FcRn			
	k_a ($M^{-1}.s^{-1}$)	k_d (s^{-1})	K_D (nM)	Chi^2
rFVIIIFc	1.6-2.7x10^6	3.4-3.7x10^{-3}	1.4-2.0	<9.0
rFIXFc	1.0-1.6x10^6	3.0-8.0x10^{-3}	3.1-5.0	>5.0
m66.6	1.5-2.0x10^6	2.0-4.2x10^{-3}	1.3-2.8	<14
VRC01	0.7-1.9x10^6	2.5-6.1x10^{-3}	3.1-5.1	<12
	Binding to murine FcRn			
	k_a ($M^{-1}.s^{-1}$)	k_d (s^{-1})	K_D (nM)	Chi^2
rFVIIIFc	1.0x10^6	2.3-2.8x10^{-4}	0.2-0.3	<3.4
rFIXFc	0.25-1.4x10^6	2.3-6.2x10^{-4}	0.3-0.9	<8.0
m66.6	0.9-1.3x10^6	2.0-3.9x10^{-4}	0.2-0.4	<14
VRC01	5.4-6.4x10^5	2.8-5.7 x10^{-}	0.4-0.9	<2.4

4

The binding kinetics of the different Fc-fused molecules and antibodies were calculated by surface plasmon resonance at pH 6 after injection of serial dilutions of Fc-fused molecules or antibodies (flow, 30 µl/min; volume, 120 µl; dissociation time, 300 s) in streptavidin-coated chips with immobilized biotinylated human or mouse FcRn at 500 RU. The values are represented as the range of 2 or 3 independent experiments.

Table 2. Hydrogen bonds and salt bridges in the interaction of FVIII C1C2 domains and FcRn

Hydrogen bonds			
Residues in C1C2 domains	**Residues in FcRn**	**Distance (Å)**	**FVIII domain**
C2021	N55	2.49	C1
R2090	S181	2.97	C1
R2090	P180	2.92	C1
K2207	D101	3.01	C2
Salt Bridges			
Residues in C1C2 domains	**Residues in FcRn**	**Distance (Å)**	**FVIII domain**
E2181	R171	1.63	C2
K2207	D101	3.01	C2

Legends to Figures

Figure 1. rFVIIIFc binds to FcRn at acidic pH. (A) Real-time interaction profiles of binding of rFVIIIFc, FIXFc, m66.6 or VRC01 to immobilized human (top) or murine (bottom) FcRn at pH 6. The black line depicts the binding profiles obtained after injection of serial dilutions of Fc-fused molecules or antibodies (25 to 0.097 nM). The red lines depict the fits of data obtained by global analysis using Langmuir kinetic model. **(B)** Values of the equilibrium dissociation constants calculated from the values of association and dissociation rate constants ($K_D=K_d/K_a$) for the binding of rFVIIIFc, FIXFc, m66.6 or VRC01 to human (blue) or murine (red) FcRn at pH 6 (Table 1). The graphs depict means ± SD (n=2 or 3). **(C)** Binding of rFVIIIFc, FIXFc, VRC01 or trastuzumab to human (left) or murine (right) FcRn by ELISA at pH 6. The Fc-fused molecules or antibodies were incubated in serial dilutions on plates coated with FcRn. The graphs depict the binding of the Fc-fused proteins or antibodies detected using a HRP-conjugated anti-human Ig Fc antibody. Binding is expressed as arbitrary units (AU) as mean ±SD based on the optical density measured at 450 nm in 2 independent experiments.

Figure 2. rFVIIIFc shows a residual binding to FcRn at neutral pH. (A) Sensorgrams of BDD-FVIII, rFVIIIFc, FIXFc, m66.6 or VRC01 binding to immobilized human (top) or murine (bottom) FcRn at pH 6 (red curves) or pH 7.4 (blue curves). Molecules were injected at 25 nM or 50 nM for pH 6 and pH 7.4,

respectively. **(B)** Heatmap showing the binding intensity of rFVIIIFc, FIXFc, m66.6 or VRC01 to human or murine FcRn at pH 7.4 by ELISA. **(C)** Binding of rFVIIIFc, FIXFc, VRC01 or trastuzumab to human (left) or murine (right) FcRn by ELISA at pH 7.4. The Fc-fused molecules or antibodies were incubated in serial dilutions on plates coated with FcRn. The graphs depict the binding of the Fc-fused proteins or antibodies detected using a HRP-conjugated anti-human Ig Fc antibody. Binding is expressed as arbitrary units (AU) as mean ±SD based on the optical density measured at 450 nm in 2 independent experiments.

Figure 3. The light chain of FVIII exhibit a positive electrostatic potential at neutral pH. (A) Structure of human anti-HIV m66.6 Fab (PDB: 4NRZ) and **(B)** of human anti-HIV VRC01-class DRVIA7 Fab (PDB: 5CD5). The heavy (VH-CH1) and light chains (VL-CL) of the human Fabs are depicted in cyan and white, respectively. **(C)** BDD FVIII structure (PDB: 6MF2). The FVIII A1, A2, A3, C1 and C2 domains are depicted in white, gray, light blue, cyan and cobalt blue, respectively. **(D)** Structure of human FcRn (PDB: 4N0F). The heavy chain of FcRn is depicted in red and the light chain β2 macroglobulin in light gray. The surface electrostatic potentials calculated using the Coulomb method (SWISS-PDB viewer) are shown at the bottom of each structure. Negative potentials are depicted in red and positive potentials in blue.

Figure 4. Positively charged residues in the C1 and C2 domains of rFVIIIFc mediate the binding of rFVIIIFc to FcRn at neutral pH. (A) The ionic strength dependence of the binding of Fc-fused molecules and antibodies to FcRn was evaluated by ELISA. Error bars indicate the SD of six $OD_{450\,nm}$ values. **(B)** Sensorgrams of the binding of rFVIIIFc alone (black curve), rFVIIIFc pre-incubated with the $F(ab')_2$ fragment of the anti-A2 IgG BOIIB2 (orange curve), the of the anti-C1 IgG KM33 (green curve), of the anti-C2 IgG BO2C11 (red curve), or with VWF (blue curve) to immobilized human (left) or murine (right) FcRn at pH 7.4. **(C)** Structure of the modelized human BDD FVIII (PDB: 6MF2) with four mutations at positions: R2090A, K2092A, F2093A, R2215A ($FVIII^{C1C2}$). The FVIII A1, A2, A3, C1 and C2 domains are depicted in white, gray, light blue, cyan and cobalt blue, respectively. Mutated resides are highlighted in red. The surface electrostatic potential of the $FVIII^{C1C2}$ mutant calculated using the Coulomb method (SWISS-PDB viewer) is shown on the right. **(D)** Protein-protein interaction of C1C2 and FcRn utilizing the HDOCK webserver. Protein structures were refined at pH 7.4 using PROPKA3.1, ProteinPrepare. The illustration shows the docked complex of C1C2 domains of FVIII in cyan and cobalt blue, respectively and FcRn containing the heavy chain depicted in red and the light chain β2 macroglobulin in light gray. Amino-acids from FcRn that are important for the Fc interaction at acidic pH (E115, E116, D130 and E133) are highlighted in green, while central amino-acids for albumin binding (W53, W59, S58, H161, H166) are highlighted in yellow. Amino-acids from FcRn and C1C2 domains that are important for biding are shown on the right. Positive (H,K,R) residues are

depicted in blue; negative (D,E) in red; neutral (S,T,N,Q) in lime; aliphatic (A,V,L,I,M) in gray, aromatic (F,Y,W) in purple, proline and glycine in orange, and cysteine in yellow.

Figure 5. Mutations in the C1 and C2 domains of FVIII moiety in rFVIIIFc decrease the binding to FcRn at neutral pH. (A) Real-time interaction profiles of $FVIII^{N2118Q}Fc$ or $FVIII^{C1C2}Fc$ with immobilized human (top) or murine (bottom) FcRn at pH 6. The black line depicts the binding profiles obtained after injection of serial dilutions of the rFVIIIFc variants (25 to 0.097 nM). The red lines depict the fits of data obtained by global analysis using Langmuir kinetic model. The values of the equilibrium dissociation constants calculated from the values of association and dissociation rate constants ($K_D=K_d/K_a$) for the binding of $FVIII^{N2118Q}Fc$ or $FVIII^{C1C2}Fc$ to human (blue) or murine (red) FcRn at pH 6 are depicted in the graph on the right (Table 1). **(B)** Sensorgrams of the binding of rFVIIIFc (black curve), $FVIII^{N2118Q}Fc$ (orange curve) or $FVIII^{C1C2}Fc$ (red curve) to immobilized human (left) or murine (right) FcRn at pH 7.4. **(C)** Binding of rFVIIIFc or rFVIIIFc variants (0.0025-5.5 nM) to human (left) or murine (right) FcRn by ELISA at pH 7.4. The Fc-fused molecules were incubated in serial dilutions on plates coated with FcRn. (**D)** Ionic strength dependence of the binding of Fc-fused FVIII variants to human (left) or murine (right) FcRn evaluated by ELISA. The graphs depict the binding of the Fc-fused proteins detected using a secondary goat $F(ab')_2$ anti-human Ig Fc conjugated to HRP. Binding is

expressed as arbitrary units (AU) as mean ± SD based on the optical density measured at 450 nm in 2 independent experiments.

Figure 6. In vivo half-life of Fc-fused FVIII half-life. (A-B) rFVIIIFc or FVIII^{C1C2}Fc were intravenously injected to FVIII-KO (A) or VWF-KO (B) mice. The residual FVIII:Ag was measured in plasma at different time points by ELISA. The data is plotted as percentage of initial FVIII:Ag (measured 5 min after injection), and as mean ± SD of 2 independent experiments (n=6 mice per group per experiment). The half-lives of rFVIIIFc variants were determined by fitting the data to a two-phase or one-phase decay curve for FVIII-KO and VWF-KO mice, respectively (Prism 9.4.1). Significant differences were assessed at each time point using the two-sided non-parametric Mann-Whitney (*$p<0.05$, **$p<0.01$).

Figure 1

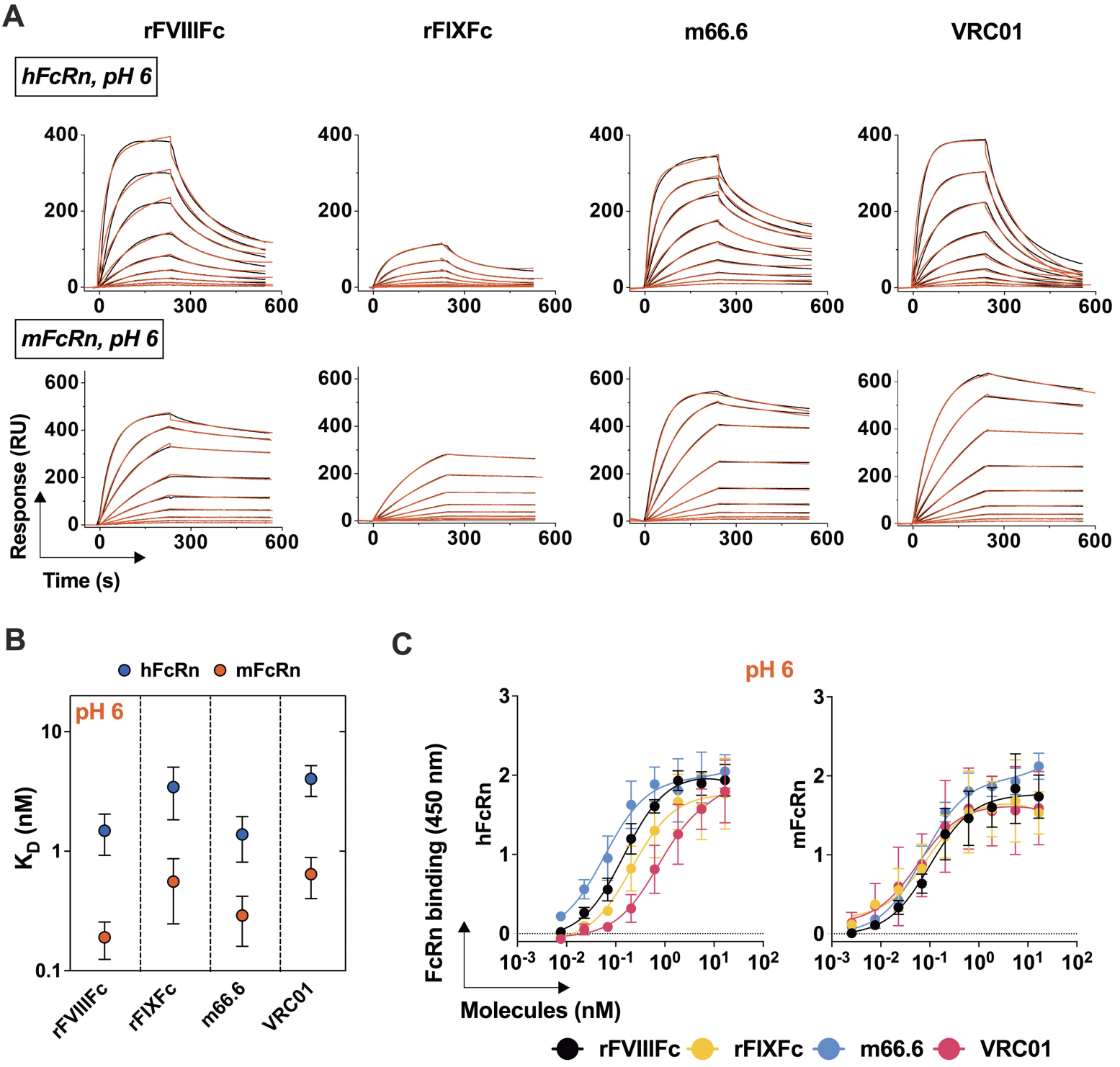
A
rFVIIIFc
rFIXFc
m66.6
VRC01
hFcRn, pH 6
mFcRn, pH 6
Response (RU)
Time (s)
B
hFcRn
mFcRn
pH 6
K_D (nM)
rFVIIIFc
rFIXFc
m66.6
VRC01
C
pH 6
hFcRn
mFcRn
FcRn binding (450 nm)
Molecules (nM)
rFVIIIFc
rFIXFc
m66.6
VRC01

Figure 2

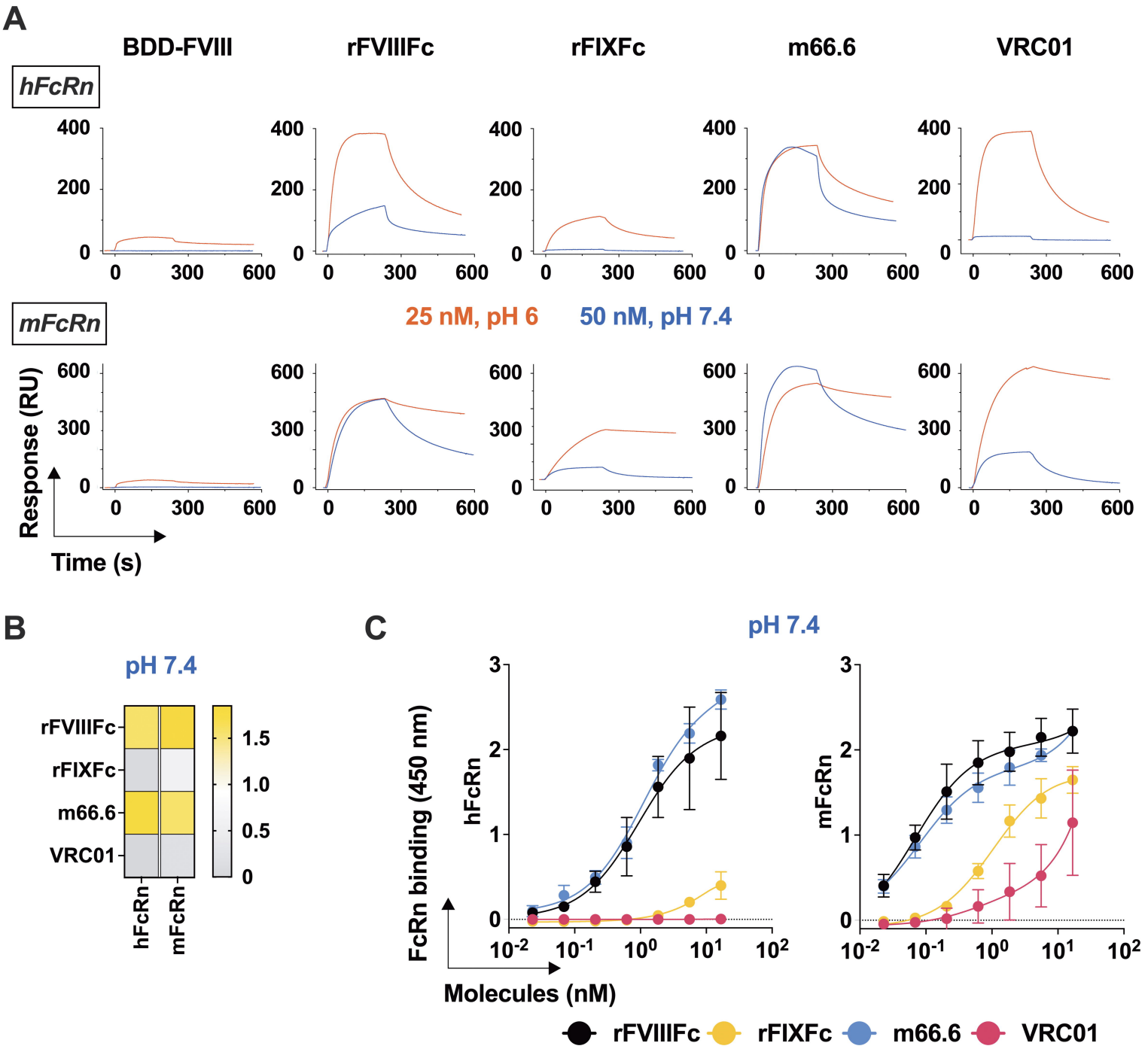
A
BDD-FVIII
rFVIIIFc
rFIXFc
m66.6
VRC01
hFcRn
mFcRn
25 nM, pH 6
50 nM, pH 7.4
Response (RU)
Time (s)
B
pH 7.4
rFVIIIFc
rFIXFc
m66.6
VRC01
hFcRn
mFcRn
C
pH 7.4
FcRn binding (450 nm)
hFcRn
mFcRn
Molecules (nM)
rFVIIIFc
rFIXFc
m66.6
VRC01

Figure 3

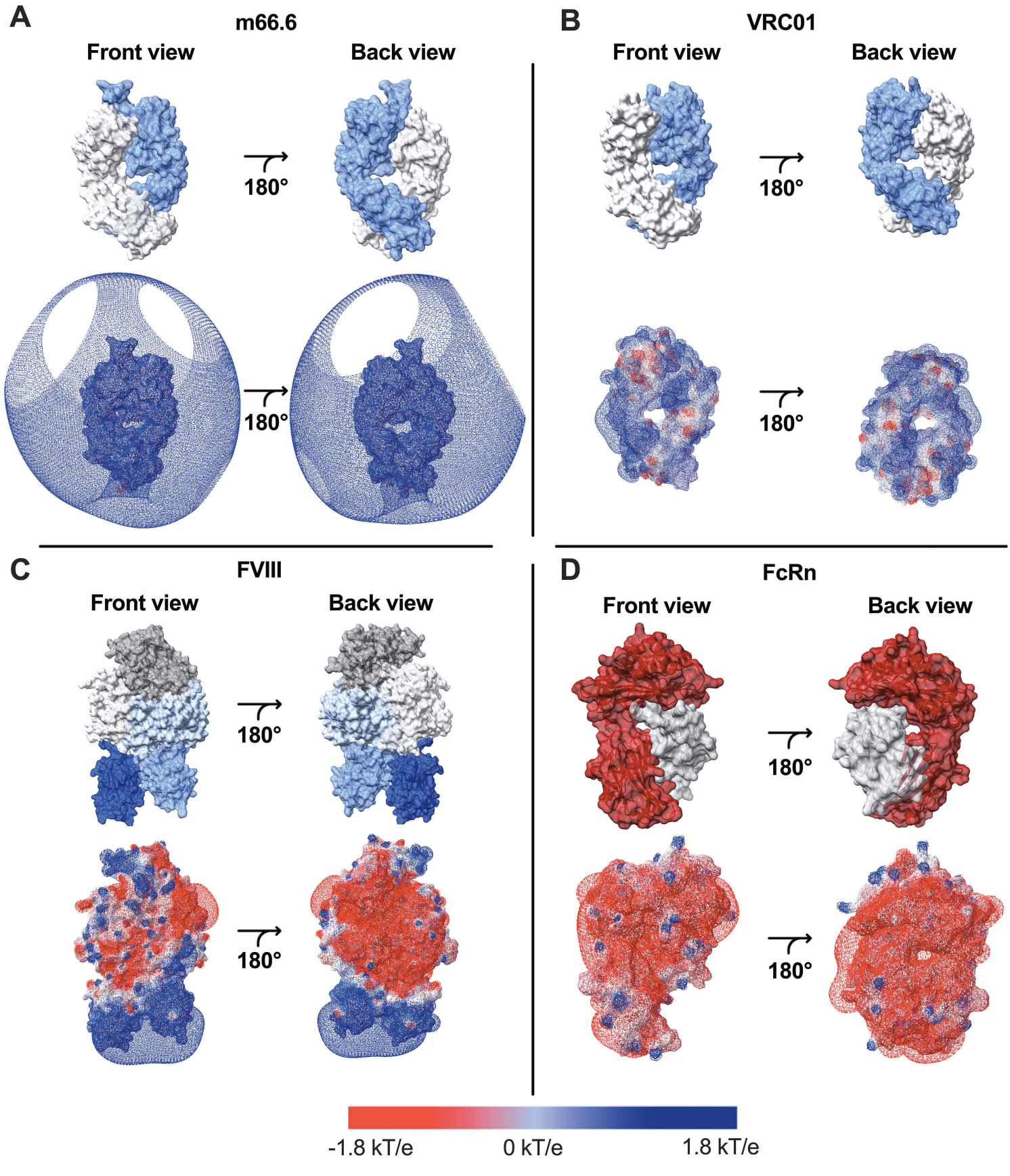
A
m66.6
Front view
Back view
180°
180°
B
VRC01
Front view
Back view
180°
180°
C
FVIII
Front view
Back view
180°
180°
D
FcRn
Front view
Back view
180°
180°
-1.8 kT/e
0 kT/e
1.8 kT/e

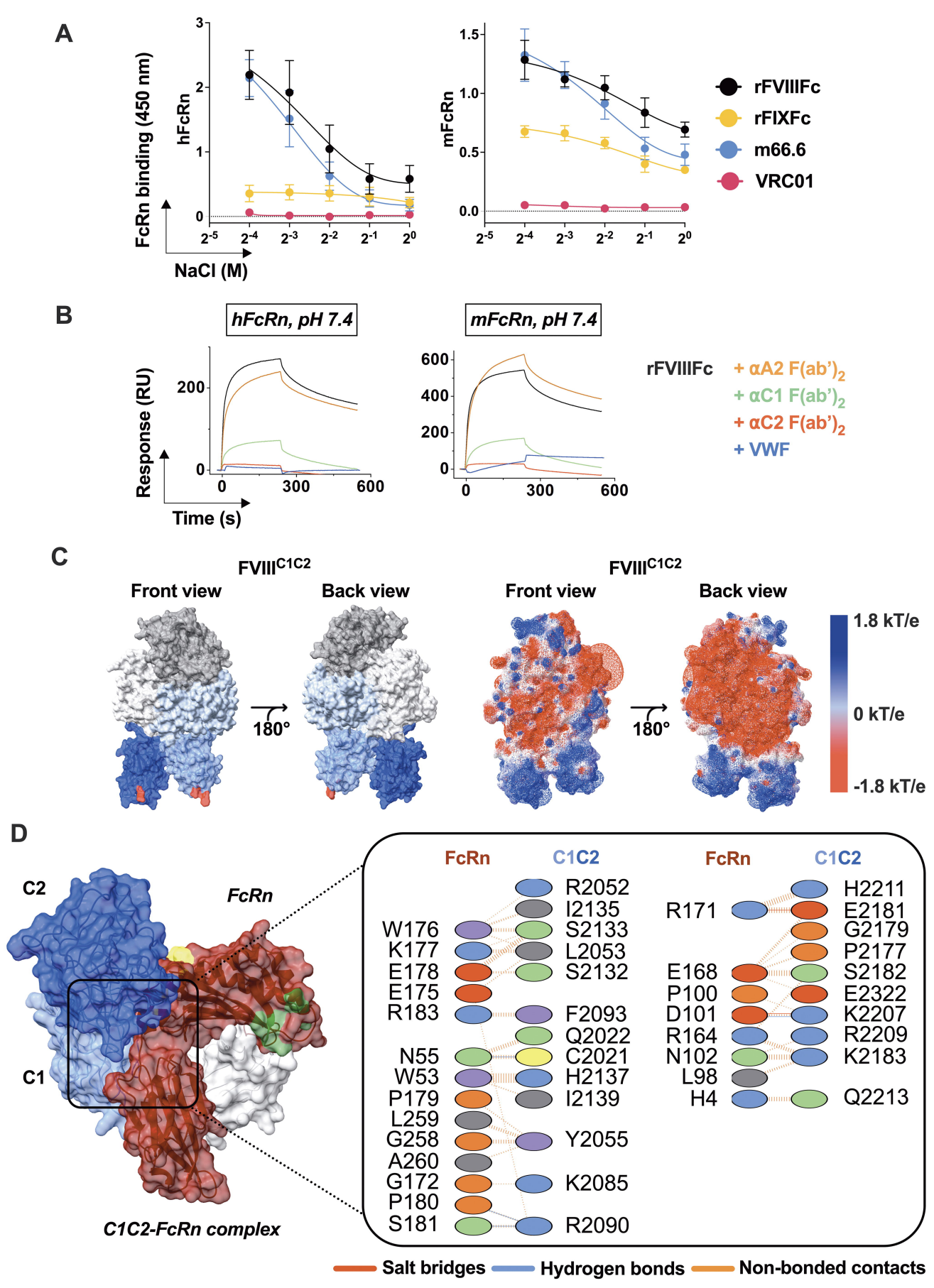
A
FcRn binding (450 nm)
hFcRn
mFcRn
NaCl (M)
rFVIIIFc
rFIXFc
m66.6
VRC01
B
hFcRn, pH 7.4
mFcRn, pH 7.4
Response (RU)
Time (s)
rFVIIIFc
+ αA2 F(ab')2
+ αC1 F(ab')2
+ αC2 F(ab')2
+ VWF
C
FVIII C1C2
Front view
Back view
180°
1.8 kT/e
0 kT/e
-1.8 kT/e
D
C2
C1
FcRn
C1C2-FcRn complex
FcRn
C1C2
W176
K177
E178
E175
R183
N55
W53
P179
L259
G258
A260
G172
P180
S181
R2052
I2135
S2133
L2053
S2132
F2093
Q2022
C2021
H2137
I2139
Y2055
K2085
R2090
R171
E168
P100
D101
R164
N102
L98
H4
H2211
E2181
G2179
P2177
S2182
E2322
K2207
R2209
K2183
Q2213
Salt bridges
Hydrogen bonds
Non-bonded contacts

Figure 5

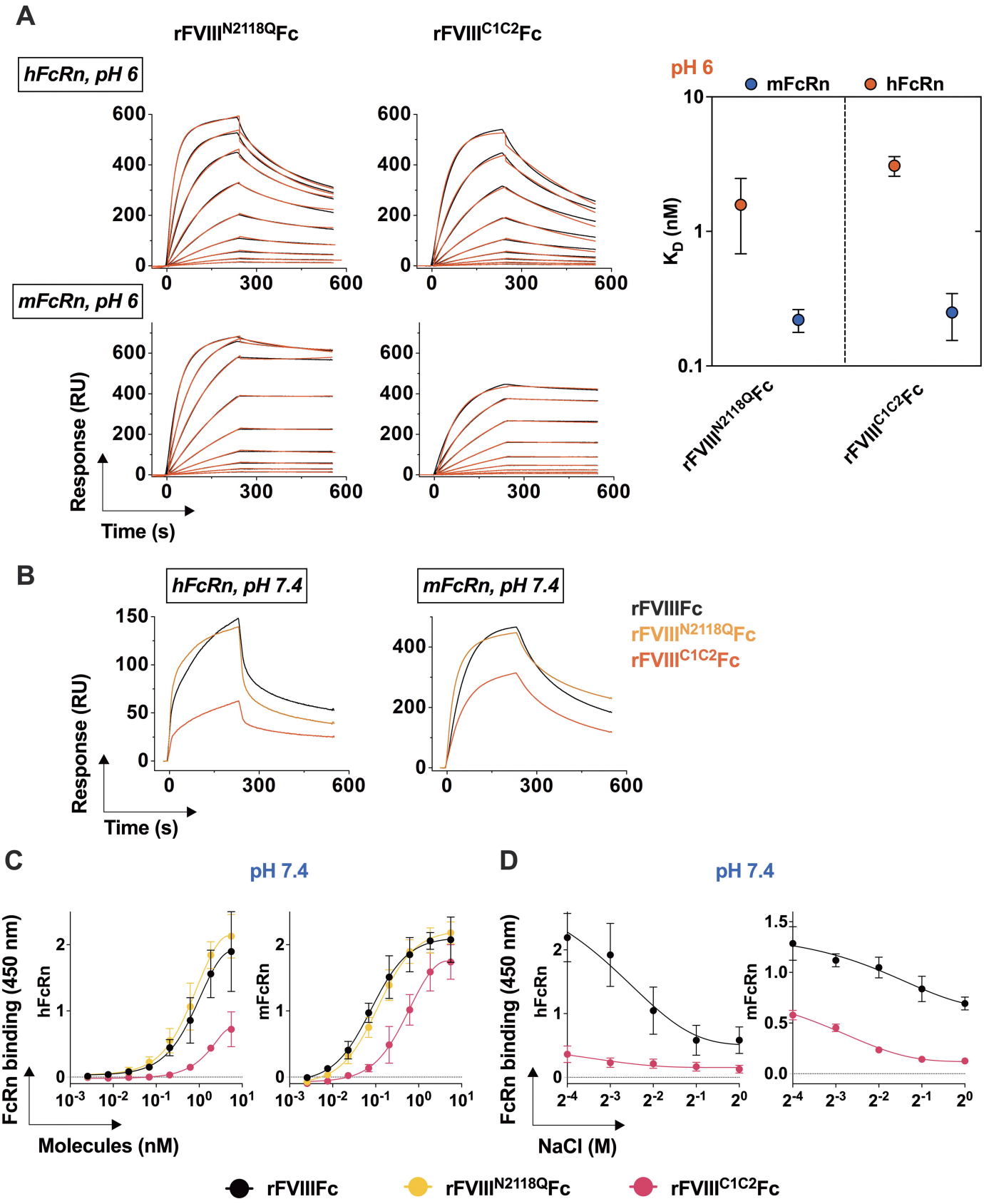
A
rFVIII^N2118QFc
rFVIII^C1C2Fc
hFcRn, pH 6
mFcRn, pH 6
Response (RU)
Time (s)
pH 6
mFcRn
hFcRn
K_D (nM)
rFVIII^N2118QFc
rFVIII^C1C2Fc
B
hFcRn, pH 7.4
mFcRn, pH 7.4
Response (RU)
Time (s)
rFVIIIFc
rFVIII^N2118QFc
rFVIII^C1C2Fc
C
pH 7.4
FcRn binding (450 nm)
hFcRn
mFcRn
Molecules (nM)
D
pH 7.4
FcRn binding (450 nm)
hFcRn
mFcRn
NaCl (M)
rFVIIIFc
rFVIII^N2118QFc
rFVIII^C1C2Fc

Figure 6

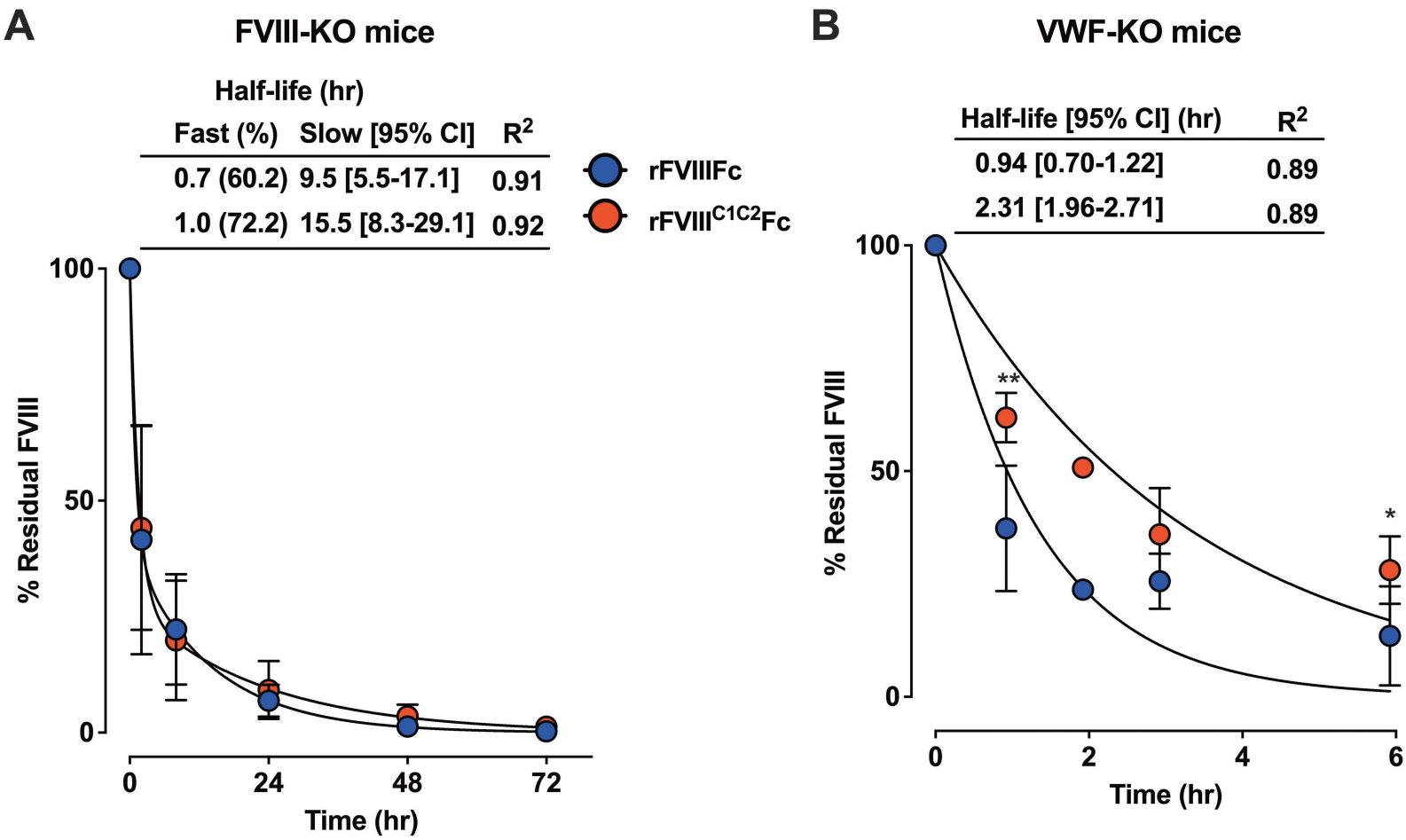
A
FVIII-KO mice
Half-life (hr)
Fast (%) Slow [95% CI] R2
0.7 (60.2) 9.5 [5.5-17.1] 0.91
1.0 (72.2) 15.5 [8.3-29.1] 0.92
rFVIIIFc
rFVIIIC1C2Fc
% Residual FVIII
100
50
0
0
24
48
72
Time (hr)
B
VWF-KO mice
Half-life [95% CI] (hr) R2
0.94 [0.70-1.22] 0.89
2.31 [1.96-2.71] 0.89
% Residual FVIII
100
50
0
**
*
0
2
4
6
Time (hr)

Supporting Information

Supplemental Methods

Sources of antibodies. Genes encoding the VL and VH regions of human anti-HIV m66.6 IgG was given by Hugo Mouquet (Institut Pasteur, France) and cloned in eukaryotic expressing vectors. The human anti-HIV VRC01-class DRVIA7 IgG expressing plasmids were obtained through the NIH AIDS Reagent Program (Division of AIDS, NIAID, at the National Institutes of Health). Antibodies were expressed in ExpiCHO cells transiently transfected with the different constructs (Thermo Scientific). After 8 days of culture in serum free conditions, supernatants were collected, and antibodies were purified by affinity chromatography (HiTrap MabSelect PrismA, GE Healthcare) using a Fast Protein Liquid Chromatography system (FPLC, Holmes Analytical). The final products were buffer-exchanged to PBS, pH 7.4 using Slide A-lyser dialysis cassettes (Thermo Scientific). Both mAbs shared an identical Fc.

FcRn binding by surface plasmon resonance. The binding of Fc-fused proteins to the human and mouse FcRn were studied by surface plasmon resonance using a Biacore 2000 (Cytiva). Biotinylated hFcRn or mFcRn (kind gift from Dr Sune Justesen, Immunitrack, Danemark) were diluted in tris-citrate buffer (100 mM Tris, 100mM NaCl, 5% glycerol and 0.1% tween 20 at pH 6 or pH 7.4) and immobilized on a streptavidin-coated sensor chip at a protein surface density of about 0.5 ng/mm^2 (450–550 RU). Fc-fused proteins were diluted in running buffer (100 mM Tris, 100 mM NaCl, 5% glycerol and 0.1% tween 20, pH 6 or 7.4) and injected at 25°C. The injections were performed using the KINJECT mode (flow,

30 µl/min; volume, 120 µl; dissociation time, 300 s). For regeneration, 15 µl of 100 mM Tris, 100 mM NaCl pH 7.8 (regeneration buffer) were injected. For calculation of binding constants at pH 6, the binding was evaluated in 2-fold serial dilutions of the samples (25 to 0.097 nM). Kinetic constants were calculated from the sensorgrams using the 1:1 Langmuir or binding with drifting baseline model of BIAevaluation software. The quality of the fitting of the models was judged by the low values of the Chi^2, not exceeding the 10% of the highest RU. The equilibrium dissociation constants were calculated from the values of association and dissociation rate constants, as $K_D=K_d/K_a$. When indicated, rFVIIIFc was pre-incubated with VWF at 1/50 FVIII/VWF ratio or 1/1 ratio of $(F(ab')_2$ fragments of anti-A2 (BOIIB2 - patent US20070065425A1), anti-C1 (KM33[1]) or anti-C2 (BO2C11[2]) monoclonal IgG at 30 min at 4°C.

FcRn binding by ELISA. Biotinylated human or murine FcRn (2 µg/mL, Immunitrack, Denmark) were immobilized on streptavidin (10 µg/mL) precoated ELISA plates (Thermo Scientific) and previously blocked with synthetic block (Thermo Scientific), 0.1% tween 20. To determine binding to FcRn, the molecules to be tested were diluted in 100 mM Tris, 100 mM NaCl, 0.1% tween 20, at pH 6 or 7.4 and added to the plate. To determine the ionic strength dependence of the binding, the molecules were tested at 2 nM or 0.2 nM, for human and murine FcRn, respectively, in 10 mM HEPES pH 7.1 containing 0, 0.06, 0.125, 0.25, 0.5, or 1 M NaCl. Bound molecules were detected with horse-radish peroxidase (HRP)-conjugated goat $F(ab')_2$ anti-human Ig (2012-05, Southern Biotech, Anaheim, CA) or, when indicated, FVIII was detected using a mouse monoclonal anti-FVIII A2

domain IgG (GMA8015, Green Mountain, Burlington, VT) and a goat anti-mouse IgG conjugated with HRP (1030-05, Southern Biotech, Birmingham, AL). The 3,3',5,5'-tétraméthylbenzidine (TMB) was used as a substrate. Optical densities were measured at 450 nm with a TECAN Infinite 200.

Evaluation of surface electrostatic potentials. The 3D structures of human FcRn (4N0F), human BDD FVIII (6MF2), human anti-HIV m66.6 Fab (4NRZ), human anti-HIV VRC01-class DRVIA7 Fab (5CD5) were obtained from the PDB database (https://www.rcsb.org/) [3]. Modeling of the $FVIII^{C1C2}$ mutant with the four R2090A, K2092A, F2093A, R2215A mutations was performed using the Iterative Threading Assembly Refinement (I-TASSER) web server (https://zhanglab.dcmb.med.umich.edu/I-TASSER/). This web-based tool utilizes homology modeling techniques to generate 3D structures based on known templates. The model then underwent quality assessment using the SAVES platform (https://saves.mbi.ucla.edu/), and their Ramachandran plot distributions were evaluated through the PDBsum server (https://www.ebi.ac.uk/thornton-srv/databases/cgi-in/pdbsum/) [4]. Subsequently, the mutant model was subjected to energy minimization using the SWISS-PDB Viewer tool (https://www.expasy.org/spdbv) to alleviate internal constraints and reduce the overall potential energy of the model [5]. The surface electrostatic potentials of the proteins and of the modelized BDD $FVIII^{C1C2}$ mutant were calculated by the Coulomb computational method using SWISS-PDB viewer.

Docking of FVIII C1C2 domains and FcRn at pH7.4. The C1C2 domains of FVIII were modeled using the crystal structure of FVIII (2R7E) as a template through the ITASSER Modelling server (https://zhanggroup.org/I-TASSER/). The structure underwent refinement using ProteinPrepare (https://playmolecule.org/proteinPrepare/), a web application designed for protein manipulation such as titration and protonation at user-specified pH levels [6]. The solvent pH was set to 7.4 to replicate physiological conditions. Utilizing PROPKA3.1, ProteinPrepare predicted protonation states of residues based on the designated pH, ensuring accurate representation. Simultaneously, the software employed PDB2PQR to optimize hydrogen-bonding networks within the protein structures, promoting stability under the specified pH conditions. The refined C1C2 and FcRn protein structures were then downloaded in PDB format for subsequent docking studies. Protein-protein docking was conducted utilizing the HDOCK webserver (http://hdock.phys.hust.edu.cn/) [7]. This computational approach explores the molecular interactions between the proteins, providing insights into complex formation and strength. Visualization of the docking results was generated using Biovia Discovery Studio and Pymol for 3D representations, while 2D visualizations were generated using PDBsum (https://www.ebi.ac.uk/thornton-srv/databases/pdbsum/) [5].

In vivo half-life of Fc-fused FVIII variants. Ten- to 15-week-old FVIII exon 16 knock-out (FVIII-KO) mice and VWF-KO mice on the C57BL/6 background were used. Animals were handled in agreement with local ethical authorities (approved

by Charles Darwin ethics committee #28694-2020121017336521). FVIII- or VWF-KO mice were intravenously injected with 1 µg rFVIIIFc (Eloctate®, Sanofi) or FVIII^{C1C2}Fc. Blood was collected in citrated tubes (Sigma Aldrich) at different time points. Plasma was prepared and kept at -80°C until use. FVIII:Ag was measured by ELISA. For this, ELISA plates were coated overnight at 4°C with 5 µg/mL mouse anti-human IgG Fc antibody (LS-C108752, LifeSpan BioSciences, Shirley, MA). Plasma diluted in PBS-5% BSA was added to the plates. Bound FVIII was detected with a biotinylated mouse monoclonal anti-FVIII A2 domain IgG (GMA8015, Green Mountain), streptavidin conjugated to horse-radish peroxidase (HRP, R&D Systems, Minneapolis, MN) and OPD (o-phenylenediamine dihydrochloride) substrate. Optical densities were measured at 492 nm with a TECAN Infinite 200.

Von Willebrand factor binding ELISA. Von Willebrand factor (VWF, Wilfactin, LFB, France) at 2 µg/mL was coated on ELISA plates (Thermo Scientific) overnight at 4°C. The rFVIIIFc variants were diluted in PBS-1% milk, 0.1% tween 20 and added to the plates. Bound molecules were detected with a biotinylated mouse monoclonal anti-FVIII A2 domain IgG (GMA8015, Green Mountain), streptavidin conjugated to HRP (R&D Systems) and TMB substrate. Optical densities were measured at 450 nm with a TECAN Infinite 200.

References

1. van den Brink EN, Turenhout EA, Bovenschen N, et al. Multiple VH genes are used to assemble human antibodies directed toward the A3-C1 domains of factor VIII. Blood 2001;97(4):966–972.
2. Jacquemin MG, Desqueper BG, Benhida A, et al. Mechanism and kinetics of factor VIII inactivation: study with an IgG4 monoclonal antibody derived from a hemophilia A

patient with inhibitor. Blood 1998;92(2):496–506.
3. Berman HM, Westbrook J, Feng Z, et al. The Protein Data Bank. Nucleic Acids Res 2000;28(1):235–242.
4. Laskowski RA, Jabłońska J, Pravda L, Vařeková RS, Thornton JM. PDBsum: Structural summaries of PDB entries. Protein Sci 2018;27(1):129–134.
5. Bhale AS, Venkataraman K. Delineating the impact of pathogenic mutations on the conformational dynamics of HDL's vital protein ApoA1: a combined computational and molecular dynamic simulation approach. J Biomol Struct Dyn 2023;41(24):15661–15681.
6. Martínez-Rosell G, Giorgino T, De Fabritiis G. PlayMolecule ProteinPrepare: A Web Application for Protein Preparation for Molecular Dynamics Simulations. J Chem Inf Model 2017;57(7):1511–1516.
7. Yan Y, Zhang D, Zhou P, Li B, Huang S-Y. HDOCK: a web server for protein-protein and protein-DNA/RNA docking based on a hybrid strategy. Nucleic Acids Res 2017;45(W1):W365–W373.

Supplemental Tables

Table S1. Non-bonded contacts between FVIII C1C2 domains and FcRn

Residues in the C1C2 domains	Residues in FcRn	Distance (Å)	FVIII domain
2021	55	2.488	C1
2021	169	4.564	C1
2022	53	4.106	C1
2022	55	3.031	C1
2023	55	4.403	C1
2052	172	3.954	C1
2052	176	3.878	C1
2052	177	4.447	C1
2053	175	3.239	C1
2053	176	3.580	C1
2053	177	2.908	C1
2055	179	3.364	C1
2055	258	2.905	C1
2055	259	2.488	C1
2055	260	3.236	C1
2085	172	3.490	C1
2085	173	4.668	C1

2087	176	4.315	C1
2090	179	4.802	C1
2090	180	2.924	C1
2090	181	2.969	C1
2090	182	4.927	C1
2092	183	4.750	C1
2093	183	3.070	C1
2094	16	4.689	C1
2095	19	4.355	C1
2130	12	4.971	C1
2130	13	4.160	C1
2131	178	4.416	C1
2131	231	4.641	C1
2131	12	3.807	C1
2131	13	3.399	C1
2132	178	2.840	C1
2133	176	2.947	C1
2133	177	3.874	C1
2133	178	2.711	C1
2133	231	4.885	C1
2135	173	4.355	C1
2135	176	3.446	C1
2137	50	4.865	C1

2137	53	2.744	C1
2137	54	4.666	C1
2138	53	4.669	C1
2139	53	3.305	C1
2157	19	4.603	C1
2163	177	4.197	C1
2176	169	4.376	C2
2177	168	3.002	C2
2178	168	4.852	C2
2179	168	3.791	C2
2180	102	4.870	C2
2181	164	4.961	C2
2181	167	4.010	C2
2181	168	3.228	C2
2181	171	1.592	C2
2182	164	3.560	C2
2182	165	3.917	C2
2182	168	2.649	C2
2183	98	2.535	C2
2183	99	4.752	C2
2183	102	2.890	C2
2183	103	4.797	C2
2183	164	2.876	C2

2187	101	4.594	C2
2187	102	4.499	C2
2206	102	4.834	C2
2207	100	3.831	C2
2207	101	2.777	C2
2209	102	3.454	C2
2210	171	4.637	C2
2211	171	3.154	C2
2211	175	3.531	C2
2213	4	2.833	C2
2213	100	4.554	C2
2214	4	4.230	C2
2214	100	4.963	C2
2215	100	4.880	C2
2215	101	4.738	C2
2322	168	3.104	C2

Table S2. Specific activities of Fc-fused FVIII variants. FVIII activity was measured by functional chromogenic assay and protein concentration was evaluated by absorbance at 280 nm.

	Specific activity (IU/mg)
rFVIIIFc	4265
rFVIII^{C1C2}Fc	1392-2398
rFVIII^{N2118Q}Fc	1951

Table S3. Kinetic parameters for the binding of FVIII^{N2118Q}Fc and rFVIII^{C1C2}Fc to human and mouse FcR at pH 6. The binding kinetics of the rFVIIIFc variants were calculated by surface plasmon resonance at pH 6 after injection of serial dilutions of Fc-fused molecules (flow, 30 µl/min; volume, 120 µl; dissociation time, 300 s) in streptavidin-coated chips with immobilized biotinylated human or mouse FcRn at 500 RU. The values are represented as the range of 2 or 3 independent experiments.

Binding to human FcRn				
	k_a ($M^{-1}.s^{-1}$)	k_d (s^{-1})	K_D (nM)	Chi^2
rFVIII^{C1C2}Fc	6.5-8.1x10^5	2.1-2.4x10^{-3}	2.6-3.6	<13
rFVIII^{N2118Q}Fc	1.2-1.6x10^6	1.7-3.0x10^{-3}	1.0-2.6	<7.0
Binding to murine FcRn				
	k_a ($M^{-1}.s^{-1}$)	k_d (s^{-1})	K_D (nM)	Chi^2
rFVIII^{C1C2}Fc	6.0-6.1x10^5	1.2-2.2x10^{-4}	0.2-0.36	<3.5
rFVIII^{N2118Q}Fc	1.0-1.2x10^6	2.1-2.9x10^{-4}	0.2-0.25	<4.0

Supplemental Figures

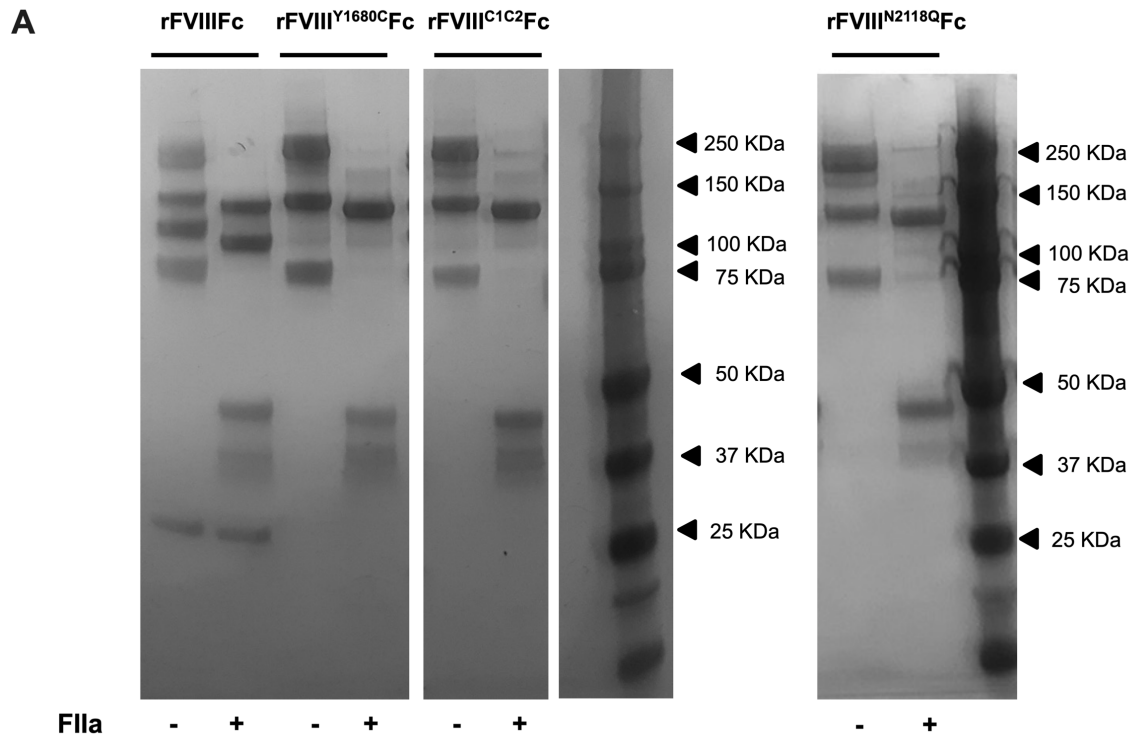

Figure S1. SDS-PAGE of rFVIIIFc, FVIII^{Y1680C}Fc, FVIII^{C1C2}Fc or FVIII^{N2118Q}Fc with and without prior exposure to thrombin (FIIa, 1U).

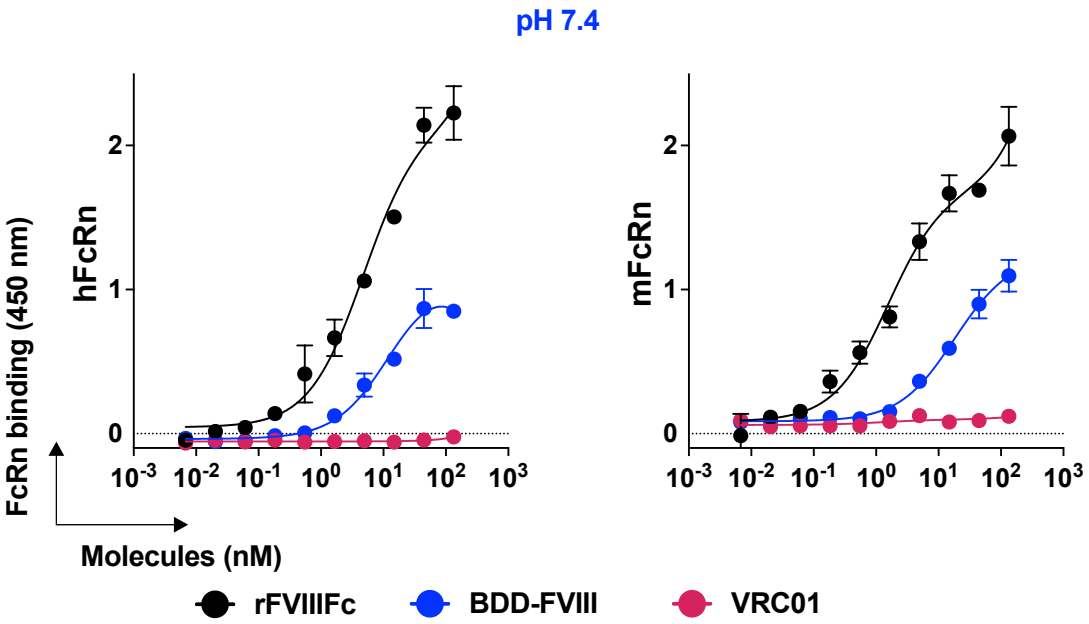

Figure S2. Binding of rFVIIIFc or BDD-FVIII (0.007-133 nM) to human (left) or murine (right) FcRn by ELISA at pH 7.4. The molecules were incubated in serial dilutions on plates coated with FcRn. The graphs depict the binding of the FVIII proteins using a mouse monoclonal anti-FVIII A2 domain IgG (GMA8015) and a goat anti-mouse IgG conjugated with HRP (1030-05). Binding is expressed as arbitrary units (AU) as mean ±SD based on the optical density measured at 450 nm in 2 independent experiments. VRC01 was used as negative control.

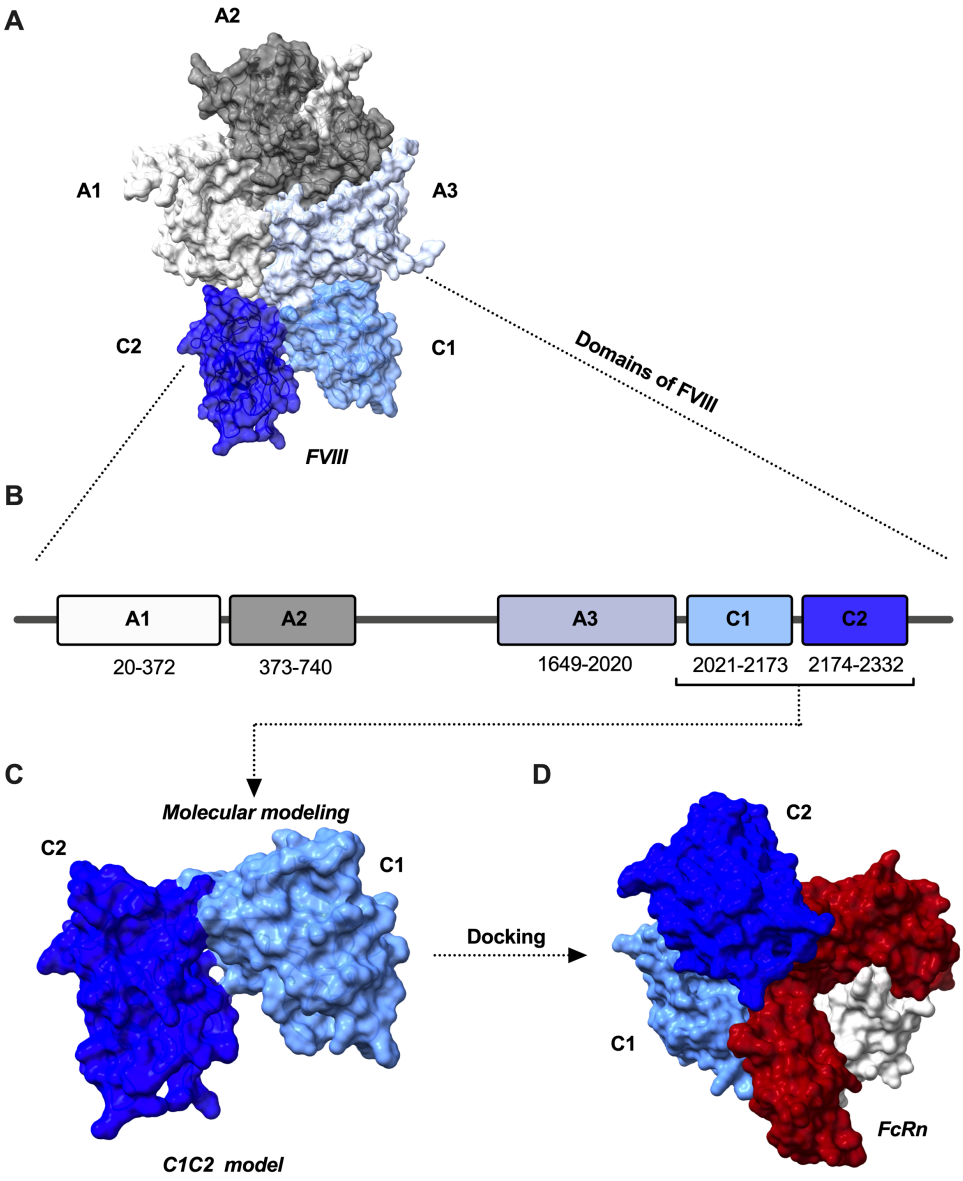

Figure S3. (A) Structure of BDD FVIII (PDB: 2R7E), the A1, A2, A3, C1 and C2 domains are depicted in white, gray, light blue, cyan and cobalt blue, respectively. **(B)** BDD FVIII consists of the heavy chain containing the A1 (20-372) A2 (373-740) domains, a truncated B-domain coding the 14-amino acid segment SFSQNPPVLKRHQR in place of the B domain (741-1648), and the light chain with A3 (1649-2020), C1 (2021-2173) and C2 (2174-2332) domains. **(C)** Depiction of

C1C2 domains of FVIII modeled using the crystal structure of FVIII (2R7E) as a template through the ITASSER Modelling server. The C1C2 molecular modeling was subjected to quality assessment via the Ramachandran plot using PDBsum server, which predicted 98% of the residues to be in the favored region. (D) Depiction of C1 (cyan) C2 (cobalt blue) domains of FVIII in complex with the light chain β2 macroglobulin (white) and heavy chain (red) of FcRn (PDB: 4N0F). Protein-protein docking was modelized at pH 7.4 and using the HDOCK webserver.

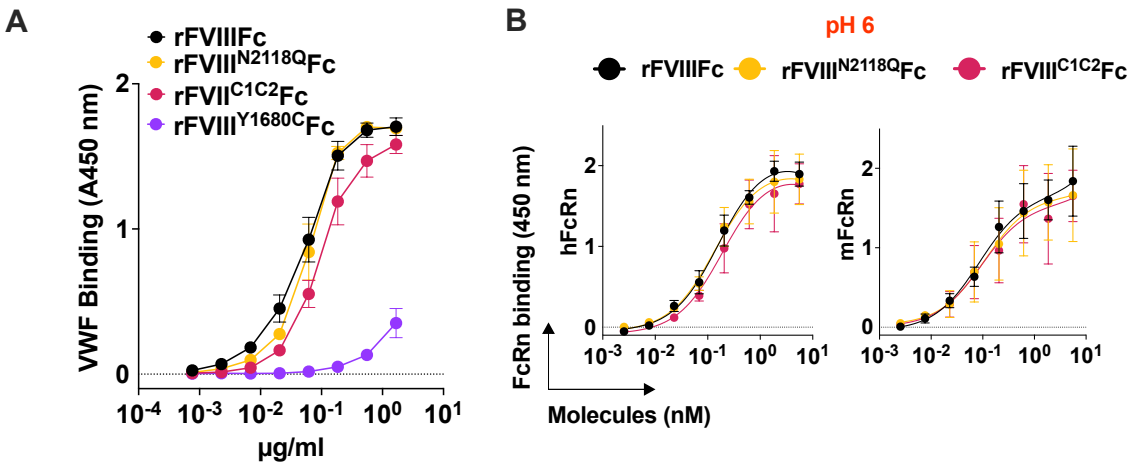

Figure S4. (A) Binding of rFVIIIFc variants to VWF by ELISA. The rFVIIIFc variants were incubated in serial dilutions on plates coated with VWF. The graphs depict the binding of the rFVIIIFc variants detected using a biotinylated mouse monoclonal anti-FVIII A2 domain IgG (GMA8015). Binding is expressed as arbitrary units (AU) as mean ± SD based on the optical density measured at 450 nm in 2 independent experiments. **(B)** Binding of rFVIIIFc or rFVIIIFc variants (0.0025-5.5 nM) to human (left) or murine (right) FcRn by ELISA at pH 6. The Fc-fused molecules were incubated in serial dilutions on plates coated with FcRn.

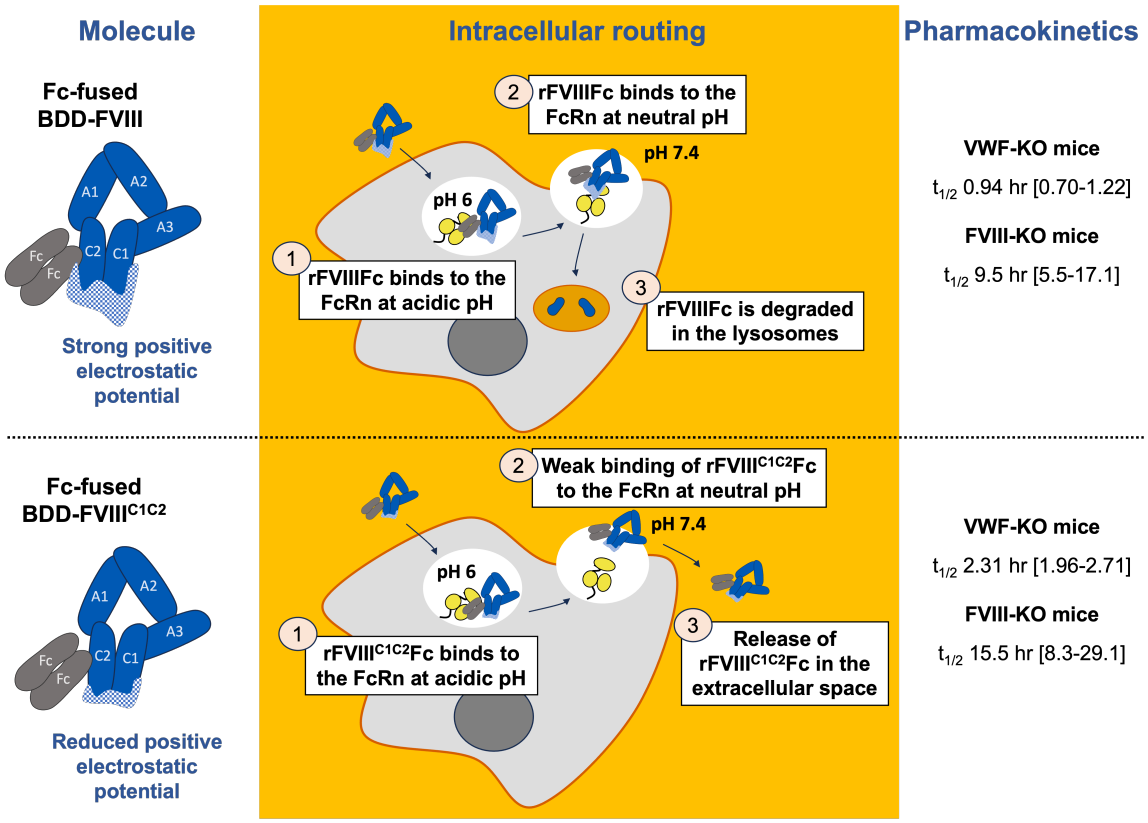

Figure S5. Visual summary. Fc-fused BDD-FVIII (rFVIIIFc) presents a strong positive electrostatic potential, mainly on the surface of the C1 and C2 domains of FVIII (left top panel). The molecule binds to the FcRn at acidic and neutral pH, which prevents the release of the molecule in the extracellular space and could foster its lysosomal degradation (central top panel). Fc-fused BDD-FVIII^{C1C2} (rFVIII^{C1C2}Fc) exhibits a reduced positive electrostatic potential (left bottom panel). The molecule binds to the FcRn at acidic pH and presents a weak binding at neutral pH, which allows its release in the extracellular space (central bottom panel). This mechanism participates in the short half-life of rFVIIIFc (right panel).